

RESEARCH ARTICLE

Open Access



Numerical estimation of a tsunami source at the flexural area of Kuril and Japan Trenches in the fifteenth to seventeenth century based on paleotsunami deposit distributions in northern Japan

Kai Sato^{1*}, Masaki Yamada², Daisuke Ishimura³, Takashi Ishizawa⁴ and Toshitaka Baba⁵

Abstract

Paleotsunami deposit investigations and numerical tsunami computations have been performed to elucidate the source and size of large tsunamis along the Kuril to Japan Trenches, particularly for unusual tsunamis that occurred in the seventeenth century, the 1611 CE Keicho tsunami (M 8.1) along the Japan Trench and seventeenth-century tsunami (> Mw 8.8) along the Kuril Trench, which caused serious damages on the coastal residents and environments. Moreover, several paleotsunami deposits dating from the thirteenth to eighteenth centuries have been reported along the area between the Kuril and Japan subduction zones, but their sources have not been clarified. In this study, we estimated the tsunami sources from numerical simulations using the distribution of fifteenth- to seventeenth-century tsunami deposits at Sekinehama along the coast of the Shimokita Peninsula. Based on numerical simulations with previously proposed fault models, the tsunami deposits showing similar ages at Sekinehama and another site on the coast of Shimokita Peninsula, which are within 50 km apart, could not be explained except with the huge earthquake models (> Mw 9.1), whose rupture zones extend to not only the Kuril or Japan Trenches but also their flexural area. Thus, we modified or newly proposed twelve fault models located in the flexural area between the two trenches to explain tsunami deposits possibly around the seventeenth century at the above-mentioned two sites on the coast of Shimokita Peninsula. Simulations using these models elucidated that the rupture in the shallow or deep plate boundaries with > 14–32 m slip (> Mw 8.55–8.76) is necessary. If the tsunami deposits around the seventeenth century along the Iburi–Hidaka coast in Hokkaido and those at the two sites mentioned above might be left by an identical event, an interplate earthquake with > 18–40 m slip (> Mw 8.62–9.2) in the flexural area is needed. Moreover, this interplate earthquake might have occurred in the deep plate boundary than in the shallower plate boundary based on slip deficit and slow earthquake distribution data. Our results offer significant insights into a large earthquake (> M 8) along the Kuril and Japan Trenches in the fifteenth to seventeenth century.

Keywords: Interplate earthquake, Computational tsunami propagation, 1611 CE Keicho tsunami, Seventeenth-century tsunami, Paleotsunami deposit, Slow earthquake

*Correspondence: k.sato16@eps.s.u-tokyo.ac.jp

¹ Department of Earth and Planetary Science, The University of Tokyo, 7-3-1 Hongo, Bunkyo-ku, Tokyo 113-0033, Japan
Full list of author information is available at the end of the article

1 Introduction

On March 11, 2011, a large tsunami associated with a megathrust earthquake along the Japan Trench (Mw 9.0; Japan Meteorological Agency 2012) induced severe damage on the north to central Pacific coast (PC) of Japan. Large amounts of tsunami deposits were left on the coastal lowlands along the PC in the Tohoku region. Knowledge gained by investigating them has yielded significant advances for tsunami deposit research and numerical modeling of tsunamis along the PC of the Tohoku region (e.g., Goto et al. 2011, 2012, 2021; Naruse and Abe 2017; Abe et al. 2020; Mitra et al. 2020; Sugawara 2021). The sources of historical tsunamis have been numerically simulated based on information obtained from tsunami deposits (e.g., Satake et al. 2008; Sugawara et al. 2012; Namegaya and Satake 2014; Ioki and Tanioka 2016). The 2011 CE Tohoku-oki tsunami and associated studies showed the relevance of geological data to evaluate the sources and sizes of past large earthquakes and tsunamis.

Paleotsunami deposits have been studied for three decades along the Japan and Kuril Trenches (e.g., Abe et al. 1990; Minoura and Nakaya 1991; Hirakawa et al. 1998; Nanayama and Shigeno 1998; Nanayama et al. 2002, 2003, 2007; Sawai et al. 2012, 2015; Ishimura and Miyauchi 2015, 2017; Takada et al. 2016; Ishizawa et al.

2022). These studies have revealed paleotsunami sources, sizes, and recurrences generated by repeating interplate earthquakes in geological time scales along the Kuril to Japan Trenches. The latest paleotsunami deposits widely distributed along the PC of the Tohoku region are thought to be associated with the 1611 CE Keicho tsunami ($>M$ 8.1; Table 1) based on geological and historical records (e.g., Sawai et al. 2012; Ebina and Imai 2014; Takada et al. 2016; Fig. 1). Although this tsunami's source is believed to be along the central Japan Trench (e.g., Hatori 1975), some concerns regarding its nature have been raised recently (e.g., Okamura and Namegaya 2011; Tetsuka et al. 2020; Ishizawa et al. 2022). Okamura and Namegaya (2011) proposed that this large tsunami event occurred along the Kuril Trench ($>M$ w 8.9) and significantly affected the PC of eastern Hokkaido and the Sanriku coast in Tohoku. To fully explain the extant historical and geological records in Tohoku and Hokkaido related to the 1611 CE Keicho tsunami event, we need to consider one huge or two to three large tsunamis along the Kuril to Japan Trenches (Tetsuka et al. 2020).

It is also known that an unusually large tsunami occurred along the Kuril Trench in the seventeenth century ($>M$ w 8.8; Ioki and Tanioka 2016) based on the distribution and age of tsunami deposits along the PC of eastern Hokkaido (e.g., Nanayama et al. 2003, 2007;

Table 1 Historical and modern tsunami list from 1611 to 2011 CE. The epicenters of each earthquake are displayed in Fig. 1

Date	Source (Tsunami name)	Epicenter (Longitude, Latitude)	Magnitude (Utsu 2004)	Tsunami height in Aomori (m)	Reference of tsunami height
11 March 2011	Off Tohoku (Tohoku-oki)	142°51.66' E, 38°06.2' N*	9.0*	2.2–2.7 (Sekinehama)	Mori et al. (2012)
26 September 2003	Off Tokachi (Tokachi-oki)	144°04.7' E, 41°46.7' N*	8.0	1.5–2.4	Tanioka et al. (2004)
4 October 1994	Off Shikotan (Shikotan-oki)	147.71° E, 43.37° N**	8.2	< 1	Watanabe (1998)
16 May 1968	Off Aomori (Tokachi-oki)	143°35' E, 40°44' N***	7.9	< 4	Watanabe (1998)
4 March 1952	Off Tokachi (Tokachi-oki)	144.13° E, 41.80° N**	8.2	< 2	Watanabe (1998)
3 March 1933	Off Iwate (Showa-Sanriku)	144.52° E, 39.23° N**	8.1	1 (Sekinehama)	Watanabe (1998)
15 June 1896	Off Iwate (Meiji-Sanriku)	144.0° E, 39.5° N**	8.2	3 (Hachinohe)	Watanabe (1998)
23 August 1856	Off Aomori (Ansei)	142.3° E, 41.0° N**	7.7	1.2–3.5	Tsuji et al. (2014)
25 April 1843	Off Nemuro (Tempo)	147.0° E, 43.0° N**	8.0	3	Tsuji et al. (2014)
29 January 1763	Off Aomori (Horeki)	142.3° E, 41.0° N**	7.7	1	Tsuji et al. (2014)
13 April 1677	Off Aomori (Empo)	142.3° E, 40.5° N**	7.9	1.5–2.9	Tsuji et al. (2014)
2 December 1611	Off Tohoku (Keicho)	144.0° E, 39.0° N**	8.1	–	–
31 June 1640	Mt. Komagatake	N/A	Related to volcanic event	–	–
19 July 1741	Oshima Ohshima	N/A	Related to volcanic event	–	–

N/A not applicable

*Japan Meteorological Agency (2012)

**Utsu (1999)

***Usami et al. (2013)

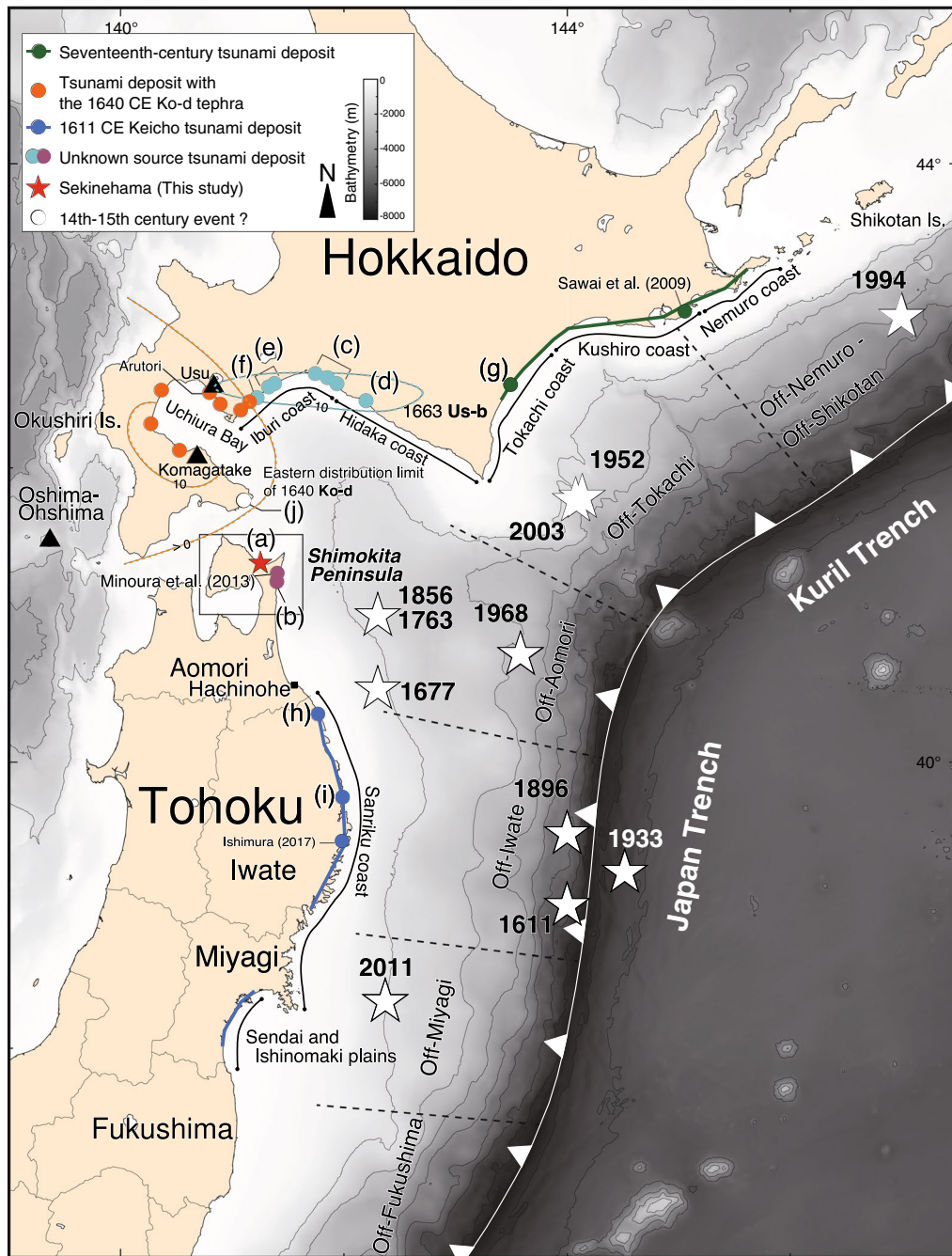


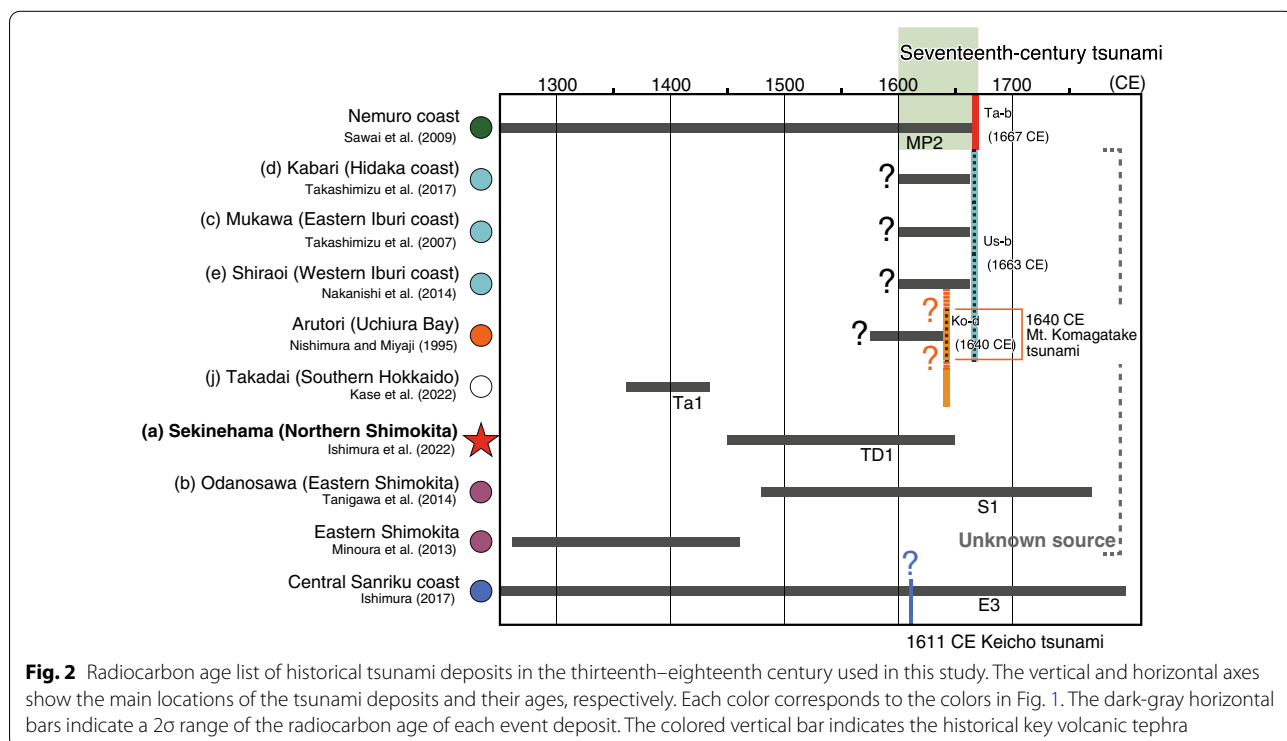
Fig. 1 Distribution map of the tsunami deposits around the seventeenth century along Kuril and Japan Trenches. The lettered color stars and circles indicate the locations of the tsunami deposits included in this study: **a** Sekinehama (Ishimura et al. 2022), **b** Odanosawa (Tanigawa et al. 2014), **c** Yufutsu–Atsuma–Mukawa (Takashimizu et al. 2007), **d** Kabari (Takashimizu et al. 2017), **e** Shiraoi (Nakanishi et al. 2014), **f** Kojohama (Nakanishi and Okamura 2019), **g** Oikamanai (Nanayama et al. 2002), **h** Harashinai (Takada et al. 2016), **i** Masaki (Takada et al. 2016), and **j** Takadai (Kase et al. 2022). The black frame indicates the Shimokita Peninsula, the white stars show the locations of historical and modern earthquake hypocenters (see Table 1 for detail), and the orange and light blue dashed lines show the thickness distribution of the 1640 CE Ko-d tephra (10 cm and > 0 cm contour lines) and 1633 CE Us-b tephra (10 cm contour line) (Nakamura 2016), respectively. The gray lines are bathymetric contour lines drawn at 1000 m intervals. The grayscale bar indicates bathymetry. The plate boundary was adapted from Iwasaki et al. (2015)

Sawai et al. 2009; Fig. 1). Tsunami deposits overlaid Ko-d tephra (1640 CE; Nakamura 2016) are distributed along Uchiura Bay, southwestern Hokkaido, and were left by a large tsunami associated with the 1640 CE Komagatake collapse following the volcanic eruption (e.g., Nishimura and Miyaji 1995; Nakanishi and Okamura 2019; Fig. 1). Tsunami deposits around the seventeenth century were also identified around the Iburī–Hidaka coast in southwestern Hokkaido (e.g., Nishimura and Miyaji 1995; Takashimizu et al. 2007, 2017; Nakanishi et al. 2014; Fig. 1), but it is still uncertain whether they are related to the 1611 CE Keicho tsunami along the Japan Trench and seventeenth-century tsunami along the Kuril Trench or entirely another tsunami source. There are other possibilities that they were formed by the tsunamigenic eruptions that occurred at Mt. Komagatake in 1640 CE (Nakanishi and Okamura 2019).

As described above, the coastal area along the Kuril and Japan Trenches experienced several tsunamis in the seventeenth century (Table 1), making it difficult to determine the source of each tsunami deposit and evaluate the sizes of past tsunamis. However, no tsunamis more than 4 m in height have been recorded to have reached around the study area in the PC of Aomori in the past 400 years (Table 1), and it is unclear whether large tsunamis have struck the coastal area in Aomori Prefecture based on historical documents. Along the east coast of

Shimokita Peninsula on the northern PC of Aomori, facing the Kuril and Japan Trenches, paleotsunami deposits were studied at two locations by Minoura et al. (2013) and Tanigawa et al. (2014) (pink circles in Fig. 1). They identified several tsunami deposits, but their sources have not been revealed. Ishimura et al. (2022) newly reported a tsunami deposit dated to the fifteenth to seventeenth century at Sekinehama on the north coast of Shimokita Peninsula (red star, Fig. 1a). Because this site is located in the flexural area between the Kuril and Japan Trenches, its source estimation can provide insights into the source problem of the large tsunami that occurred near the seventeenth century (Fig. 2).

In this study, we performed numerical tsunami simulations using twelve previously reported fault models along the Kuril and Japan Trenches, six modified previously proposed models, and six newly developed fault models with three strikes at the flexural area. We evaluated the tsunami source and its minimum tsunami size by comparing the computed tsunami inundation area with the distribution of tsunami deposits at Sekinehama along the north coast of Shimokita Peninsula in the northernmost part of the Tohoku region as well as the surrounding previous study sites. Moreover, this study is a pair work with Ishimura et al. (2022), which discusses the paleotsunami history at Sekinehama based on tsunami deposits.



2 Previously reported tsunami deposits and associated source models in the seventeenth century

2.1 Tsunami deposits along the east coast of Hokkaido from the seventeenth-century tsunami

Tsunami deposits formed by the seventeenth-century tsunami were identified on coastal areas along the Tokachi, Kushiro, and Nemuro coasts in eastern Hokkaido (green line and circle in Fig. 1) and northern territories. They are distributed about 1–4 km inland (e.g., Nanayama et al. 2002, 2003, 2007) and can be explained by multisegment interplate earthquake models (Satake et al. 2008; Ioki and Tanioka 2016; Fig. 3a and Table 2). Sawai et al. (2009) identified 15 sandy tsunami deposits during the last 6000 years, including the seventeenth-century tsunami event on the Nemuro coast of Hokkaido (Figs. 1 and 2). Along the Tokachi coast, the seventeenth-century tsunami deposit was recorded to be located up to an 18 m high cliff (Fig. 1g; Hirakawa et al. 2005). It can be explained by the T10N5S25 model proposed by Ioki

and Tanioka (2016), which has multisegment ruptures on both the shallow and deep parts of the plate interface (>Mw 8.8; Fig. 3a and Table 2). Their model yielded lower computed tsunami heights of less than 4 m on the Sanriku coast; hence, it was assumed to not cause severe damage (Ioki and Tanioka 2016). Their simulation results showed that the seventeenth-century tsunami that formed tsunami deposits along the eastern PC of Hokkaido was different from the 1611 CE Keicho tsunami that caused casualties in the Tohoku district.

2.2 Tsunami deposits in Uchiura Bay and western Iburi coast from the 1640 CE eruption of Mt. Komagatake

Along Uchiura Bay and the western part of the Iburi coast, tsunami deposits formed in the seventeenth century are distributed on the coastal area (e.g., Nishimura and Miyaji 1995; Nakanishi and Okamura 2019; orange circles in Fig. 1). They are directly covered by or with the Ko-d tephra (1640 CE; Nakamura 2016), implying that they were probably formed by a tsunami associated

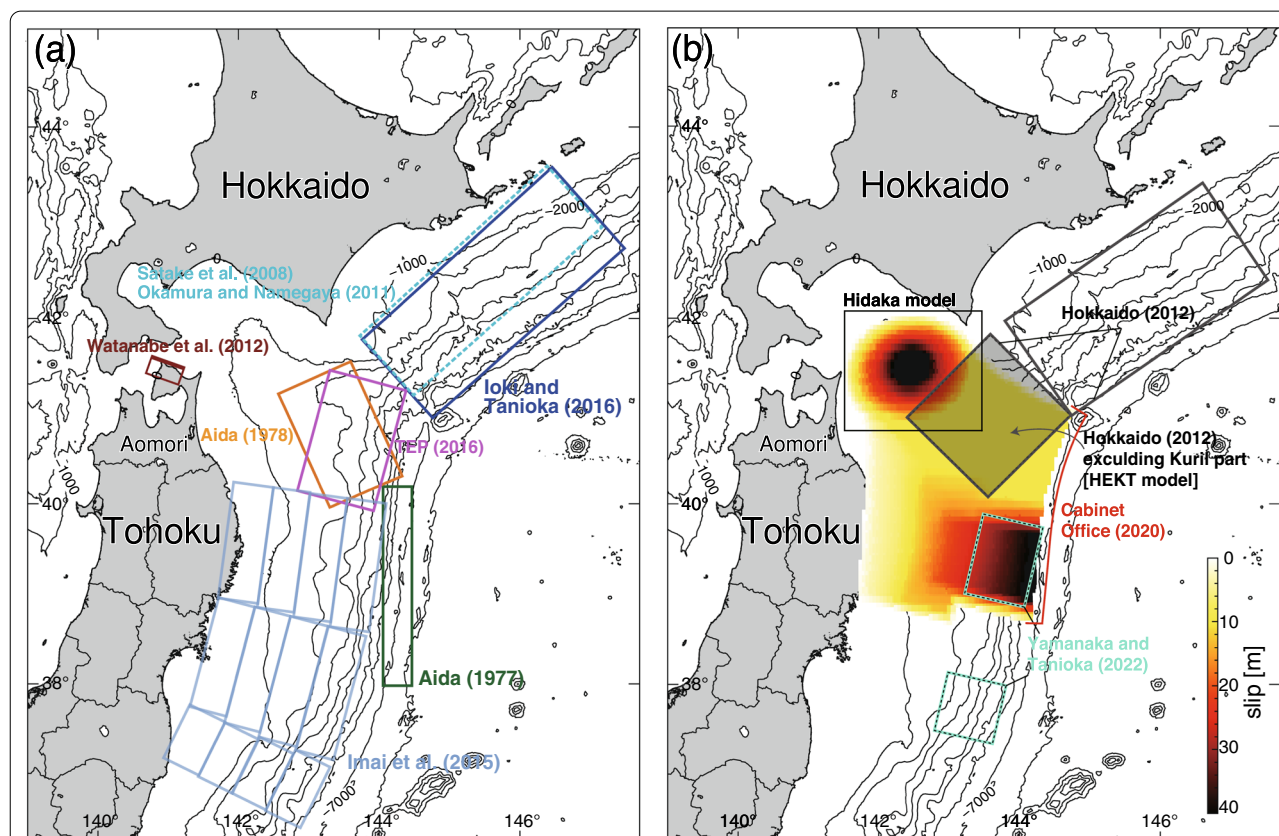


Fig. 3 Previously proposed fault models used in this study. **a** The eight fault models of the historical tsunami (Aida 1977, 1978; Satake et al. 2008; Okamura and Namegaya 2011; Watanabe et al. 2012; Imai et al. 2015; Ioki and Tanioka 2016; Tohoku Electric Power 2016). **b** One historical tsunami model (Yamanaka and Tanioka 2022), two disaster prevention models (Hokkaido Disaster Prevention Council 2012; Cabinet Office 2020), and modified previously proposed models (i.e., HEKT and Hidaka models). The color bar in **b** shows the slip amount of the Cabinet Office (2020) model. See Table 2 for details. The gray lines are bathymetric contour lines drawn at 1000 m intervals

Table 2 Fault parameters of previously proposed fault models used in this study

Fault model	Tsunami name	Subfault model	Depth (km)	Length (km)	Width (km)	Dip (°)	Strike (°)	Rake (°)	Slip (m)	Mw	Assumed rigidity (GPa)
Aida (1977)	1611 CE Keicho	N/A	0	245	50	45	180	270	8	8.3	30
Aida (1978)	1668 CE Tokachi-oki	N/A	1	150	100	20	156	38	4	8.2	40
Satake et al. (2008)	Seventeenth century	N	17	200	100	20	228	90	5	8.5	40
Okamura and Namegaya (2011)	Identical event†	T	17	100	100	20	228	90	10	8.9	40
Hokkaido Disaster Prevention Council (2012)	N/A	N	17	200	100	20	228	90	15	8.9	40
		T	17	100	100	20	228	90	30	9.2	40
		1–4	5	280	70	10	235	90	35	9.2	40
		5–6	5	140	70	10	225	90	35		
		7–10	17	280	70	20	235	90	30		
		11–12	17	140	70	20	225	90	30		
Watanabe et al. (2012)	N/A	F1	0.2	40.5	3	45	N/A	90	5	N/A	N/A
		F2	2.12	40.5	20	15	N/A	90	5		
Imai et al. (2015) Case 1	1611 CE Keicho	11	34.11	N/A	50	22	N/A	86	7.5±3.5	8.4–8.7	30
		12	19.49	N/A	50	17	N/A	86	7.0±3.1		
		13	9.09	N/A	50	12	N/A	86	5.5±2.9		
		14	3	N/A	50	7	N/A	86	7.0±3.4		
		21	34.11	N/A	50	22	N/A	86	7.3±3.1		
		22	19.49	N/A	50	17	N/A	86	5.4±2.2		
		23	9.09	N/A	50	12	N/A	86	4.5±2.1		
		24	3	N/A	50	7	N/A	86	6.9±2.9		
		31	34.11	N/A	50	22	N/A	86	3.9±1.8		
		32	19.49	N/A	50	17	N/A	86	1.7±0.9		
		33	9.09	N/A	50	12	N/A	86	3.3±1.8		
		34	3	N/A	50	7	N/A	86	16.8±1.7		
Ioki and Tanioka (2016)	Seventeenth century	N	14	200	100	15	228	90	5	8.8	40
		T	14	100	100	15	228	90	10		
		S	6.7	300	30	15	228	90	25		
Cabinet Office (2020)	Sanriku-Hidaka model	3111 subfaults	–	–	–	–	–	–	14,755 (Average)	9.1	46.3
Yamanaka and Tanioka (2022)	1611 CE Keicho	N	0	100	75	8	193	81	20	8.5	20
		S	0	75	75	8	193	81	30		
Tohoku Electric Power (2016)	1668 CE Tokachi-Oki	N/A	6	150	100	20	195	76	6.9	8.4	50

Table 2 (continued)

Fault model	Tsunami name	Subfault model	Depth (km)	Length (km)	Width (km)	Dip (°)	Strike (°)	Rake (°)	Slip (m)	Mw	Assumed rigidity (GPa)
Nakanishi and Okamura (2019)	1640 CE Komagatake	N/A	Initial water level=110 m	–	–	–	–	–	–	8.2 (Tsunami Magnitude, Mt)	

N/A not applicable

†Regard the 1611 CE Keicho tsunami as the Seventeenth-century tsunami

with the 1640 CE Mt. Komagatake eruption (Nishimura and Miyaji 1995; Nakanishi and Okamura 2019; Fig. 2). The eastern distribution limit of the tsunami deposits formed by its event is unclear because they were identified based on the existence of the overlying or including Ko-d tephra that was found today (dashed orange line in Fig. 1). Nakanishi and Okamura (2019) estimated the tsunami size that can mainly explain the tsunami deposit distributions. The maximum size is displayed in Table 2. This case is assumed to be a simplified tsunami model, not reproducing the sediment inflow following the collapse of Mt. Komagatake after the volcanic eruption, to recover the above-mentioned tsunami deposits (orange circles, Fig. 1) and the deposits on the eastern Iburi to Hidaka coasts where no Ko-d tephra was found directly above (Fig. 1c, e, and f). According to their geological investigations and numerical calculations, it is possible that sandy deposits overlaid by the volcanic tephra in the seventeenth century along Uchiura Bay and the Iburi coast (orange and light blue circles in Fig. 1) were left by the 1640 CE Mt. Komagatake eruption and tsunami.

2.3 Tsunami deposits and trace heights along the Sanriku coast from the 1611 CE Keicho tsunami

The tsunami deposits possibly formed by the 1611 CE Keicho tsunami are distributed along the Sanriku coast and Sendai and Ishinomaki plains in the Tohoku region (e.g., Sawai et al. 2012, 2015; Ishimura and Miyauchi 2015; Takada et al. 2016; Ishimura 2017; Ishizawa et al. 2022; royal blue circles and lines, Figs. 1 and 2). Most of the tsunami deposits formed by the 1611 CE event probably have been removed by artificial modification after 1611 CE; however, tsunami trace heights have been reported by reevaluating historical materials (e.g., Hatori 1975; Tsuji and Ueda 1995; Ebina and Imai 2014). The trace heights exceeded 3 m at most sites along the Sanriku coast, Sendai and Ishinomaki plains, and northern PC of Fukushima (Hatori 1975; Tsuji and Ueda 1995; Tsuji et al. 2011, 2012; Ebina and Imai 2014). Among them, the heights reached over 20 m in the central part of the Sanriku coast (Ebina and Imai 2014).

The sources of the 1611 CE Keicho tsunami (> Mw 8.3–8.7) (Aida 1977; Imai et al. 2015; Yamanaka and Tanioka 2022; Fig. 3 and Table 2) were mainly estimated based on the surveyed tsunami trace heights (e.g., Hatori 1975; Tsuji and Ueda 1995; Tsuji et al. 2011, 2012; Ebina and Imai 2014). The historical record of the 1611 CE Keicho tsunami has various interpretations, such as the possibility that the tsunami affected the PC of southern Hokkaido (Nishimura et al. 2020). Yamanaka and Tanioka (2022) proposed a tsunami earthquake model (Mw 8.5) which can explain the local flooding mechanism of the 1611 CE tsunami at a high

elevation (28.8 m) on the Central Sanriku coast. This model consisted of two fault segments near the Japan Trench axis that are far from each other, namely Off Sanriku (source N) and Off Sendai (source S) (Fig. 3b and Table 2). It yielded many short-wave components and local intensification. Okamura and Namegaya (2011) considered the 1611 CE Keicho tsunami as the seventeenth-century tsunami along the Kuril Trench partly because the tsunami arrival time on the Sanriku coast, which was inferred from the historical record of the 1611 CE Keicho tsunami, was approximately 4 h after the largest ground shaking generated by an earthquake (Tsuji and Ueda 1995), and the impact of this tsunami might have extended to the PC of Hokkaido. Their tsunami sources are placed in the same location as the T10N5 model (Satake et al. 2008) and have thrice as much slip as the T10N5 model (Fig. 3a and Table 2). The calculated tsunami heights can explain the trace heights of the 1611 CE Keicho tsunami along the Sanriku coast and Sendai plain except for sites with over 20 m elevations on the Sanriku coast.

2.4 Tsunami deposits along the eastern Iburi and Hidaka coasts of southern Hokkaido from the tsunami around the seventeenth century

There are also tsunami deposits formed in the seventeenth century along the eastern part of the Iburi to Hidaka coasts (e.g., Takashimizu et al. 2007, 2017; Nakanishi et al. 2014; light blue circles in Fig. 1). They are overlain by the 1663 CE Us-b tephra layer (dashed light blue line; Nakamura 2016) with a thinner peat layer in-between (Takashimizu et al. 2007, 2017; Nakanishi et al. 2014; Nakanishi and Okamura 2019; Fig. 2). Although this stratigraphy implies that the tsunami deposits were formed in the seventeenth century, their tsunami sources have not been determined. Among the previously proposed models, the Hokkaido (2012) model (Mw 9.2; Hokkaido Disaster Prevention Council, Hokkaido 2012; Fig. 3b and Table 2) and the Cabinet Office (2020) model (Sanriku-Hidaka model; Fig. 3b and Table 2) can explain these tsunami deposits. These rupture areas of both models are extended to the area between the Kuril and Japan Trenches. Tetsuka et al. (2020) highlighted a similar point about the Hokkaido (2012) model, implying that there might have been multiple large tsunamis at short intervals along the Kuril to Japan Trenches in the seventeenth century. Nishimura et al. (2020) highlighted that the tsunami deposits at three sites (i.e., Shadai at Shiraoi and Yufutsu and Mukawa on the Iburi coast) (Fig. 1c and e) were formed by the 1611 CE Keicho tsunami based on the absence of a 1640 CE Ko-d tephra above them and their radiocarbon ages.

2.5 Tsunami deposits on the Shimokita Peninsula from the tsunami in the thirteenth–eighteenth century

On the east coast of Shimokita Peninsula (pink circles, Fig. 1), Tanigawa et al. (2014) identified the tsunami deposit with a radiocarbon age of 1480–1770 CE (fifteenth to eighteenth century; Fig. 2) at Odanosawa (Fig. 1b). The previously proposed 1611 CE Keicho tsunami model (Imai et al. 2015) might be underestimated because they did not consider the tsunami deposit distribution at Odanosawa, possibly formed by the 1611 CE event (Tetsuka et al. 2020). Minoura et al. (2013) identified a parallel-laminated sandy tsunami deposit within dune sediments in the Sarugamori dune. They were thought to be deposited after 1269–1290 CE and before 1380–1460 CE based on radiocarbon dating (Fig. 2). As for the tsunami deposit at Sekinehama (red star, Fig. 1a), which we attempt to explain by numerical simulations in this study, Ishimura et al. (2022) identified five sandy tsunamis deposits in the last 6000-year sedimentary record. The latest one was dated to be 500–300 cal yr BP (1450–1650 CE; Fig. 2) and could be traced 200–400 m inland.

Although the source of the above tsunami deposits at the three locations has not been clarified, their ages indicate that they were probably formed by the same event that occurred between the thirteenth and eighteenth centuries. This age includes the above-mentioned tsunamis: the seventeenth-century tsunami, the 1611 CE Keicho tsunami, and the 1640 CE Mt. Komagatake eruption tsunami. There is also a possibility that they were formed by the 1677 CE Empo tsunami (M 7.9; Utsu 2004) sourced Off Aomori (Hatori 1975).

2.6 Tsunami deposit on southern Hokkaido

from the tsunami in the fourteenth–fifteenth century

Kase et al. (2022) reported a tsunami deposit with a radiocarbon age of 589–516 cal yr BP (fourteenth–fifteenth century) in Takadai Town, southern Hokkaido (white circle, Figs. 1j and 2). This deposit is located at an elevation of about 6.4 m and 200 m inland from the present shore, where the usual storm surge or typhoon could not transport sediments (Kase et al. 2022). The tsunami deposit was observed at a depth of 62 cm from the core top and was directly covered by peat (18 cm thick), with the 1640 CE Ko-d tephra at a depth of 55 cm. There were no event deposits in the peat sequence above Ko-d tephra, suggesting that no tsunami inundated there in the seventeenth century (Kase et al. 2022).

3 Methods

3.1 Preparing topography data and numerical calculations

We compiled three datasets for bathymetry data in tsunami computations. These were datasets of the Global

tsunami Terrain Model (GtTM; Chikasada 2021), M7000 digital bathymetric charts published by the Japan Hydrographic Association, and high-resolution Digital Elevation Model (DEM, 5 m and 10 m grid intervals) provided by the Geospatial Information Authority of Japan. However, we removed artificial structures located outside the present shoreline, such as sea walls and embanked roads, from the DEM data for the paleotsunami simulations. We created a nested gridded system comprising five domains with grid intervals of 18, 6, 2, 2/3, and 2/9 arcsec. The high-resolution domains gridded by 2/3 and 2/9 arcsec were defined only for Sekinehama (Fig. 1a; Ishimura et al. 2022), Odanosawa (Fig. 1b; Tanigawa et al. 2014) on the coast of Shimokita Peninsula, and Kabari (Fig. 1d; Takashimizu et al. 2017) on the Hidaka coast in southwestern Hokkaido, where paleotsunami deposits possibly formed near the seventeenth century exist. The remaining three bathymetric domains at the Iburi coast (Fig. 1c, e, and f; Takashimizu et al. 2007; Nakanishi et al. 2014; Nakanishi and Okamura 2019) did not include the high-resolution DEM because coastal topography has changed significantly since the seventeenth century (Additional file 1: Table S1). Thus, we resampled only GtTM data of 2 arcsec (50 m mesh) except for the high-resolution DEM data, for the three domains. The offshore artificial structures in the bathymetric domain of Fig. 1c on the Iburi coast were removed from GtTM data of 2 arcsec. Moreover, the combination of bathymetric data types in finer grids (2, 2/3, and 2/9 arcsec) for simulations of the sites considered in this study (e.g., Iburi and Hidaka coasts) differs for each location (see Additional file 1: Table S1 for detail). The vertical data of the bathymetric data used in this study were adopted from the present Tokyo Peil. We note that the current vertical data (e.g., tidal fluctuation, relative sea level change, and DEM data) might differ from those for the fifteenth to seventeenth century. However, we do not have enough information to fully reproduce the detailed bathymetric contours and topography at the time; therefore, we substituted the current ones following other previous paleotsunami studies (e.g., Satake et al. 2008; Yamanaka and Tanioka 2022).

Numerical tsunami calculations were performed using an open-source tsunami code called JAGURS (Baba et al. 2015), which used a finite difference scheme of staggered grid and leapfrog method with a nested algorithm. Vertical crustal deformation on the seafloor was computed using fault parameters described in the following sections by Okada's (1985) method, including a horizontal movement effect on the seafloor slope (Tanioka and Satake 1996). Kajiura's (1963) filter was applied to convert the crustal displacement to initial water elevation, which assumed

a rise time of 60 s. The Cabinet Office (2020) model described in the next subsection has 170 s of dynamic fault rupture. We performed a simulation based on it. We solved linear and nonlinear long-wave equations on the nested bathymetric domains for tsunami propagation and inundation. Numerical integration was performed for 180 min after the earthquake rupture occurrence. The time step width was 0.1 s to satisfy the stability condition of the finite difference computations. A Manning's roughness coefficient of $0.025 \text{ m}^{-1/3} \text{ s}$ was assumed in all computational domains for bottom friction. In this study, we did not perform sensitivity tests, such as Manning's roughness (e.g., Bricker et al. 2015), for simulations.

We examined a tsunami source that can explain the two sites of tsunami deposit distribution at Sekinehama and Odanosawa along the coast of Shimokita Peninsula (Fig. 1a and b) by comparing tsunami deposit distributions with calculated inundation areas because they are located close to each other (within 50 km) and show similar tsunami deposit ages: that of Sekinehama include in the fifteenth to seventeenth century (Ishimura et al. 2022) and that of Odanosawa include in the fifteenth to eighteenth century (Tanigawa et al. 2014). Then, the tsunami deposit distribution along the Iburi and Hidaka coasts, the PC of southwestern Hokkaido (Fig. 1c–f), was numerically evaluated. The details of the tsunami deposit distributions reported in the previous studies used in this study are summarized in Additional file 1: Table S1.

3.2 Fault models used in this study

The fault model parameters listed in Tables 2, 3, and 4, used for tsunami calculations, are tsunami source candidates for the tsunami deposit at Sekinehama. First, we performed numerical simulations for the source models of the 1611 CE Keicho tsunami along the Japan Trench (Aida 1977; Imai et al. 2015; Yamanaka and Tanioka 2022), the seventeenth-century tsunami along the Kuril Trench (Satake et al. 2008; Ioki and Tanioka 2016; Okamura and Namegaya 2011), the 1968 CE Tokachi-oki tsunami (Aida 1978; Tohoku Electric Power, TEP 2016) in substitution for the 1677 CE Empo tsunami, the 1640 CE Mt. Komagatake tsunami related to the volcanic eruption (Nakanishi and Okamura 2019), and a tsunami related to submarine active fault movements (Watanabe et al. 2012) (Fig. 3 and Table 2).

In addition, the Hokkaido (2012) model (Mw 9.2) and the Cabinet Office (2020) models (Case 2 of Sanriku-Hidaka model; Mw 9.1) are disaster prevention models with rupture zones that are placed not only in the Kuril and Japan Trenches, respectively, but also in the flexural area between these two trenches (Fig. 3b; Table 2). These models can explain tsunami deposits along the Iburi to Hidaka coasts in southwestern Hokkaido (Hokkaido 2012; Cabinet Office 2020).

The 1968 CE Tokachi-oki tsunami model was substituted for the 1677 CE Empo tsunami model because these two tsunamis are considered to have a similar tsunami source (e.g., Hatori 1975) and no model for

Table 3 Fault parameters of two modified previously proposed models

Model name	Subfault	Slip (m)	Mw*	
HEKT model: Hokkaido (2012) model excluding Kuril Trench part				
HEKT (base)	5–6	35	8.87	
	11–12	30		
HEKT-1	5–6	25	8.76	
	11–12	20		
HEKT-2	5–6	15	8.59	
	11–12	10		
Model name	Maximum slip (m)	Average slip (m)	Fault slip factor	Mw*
Hidaka model: Cabinet Office (2020) model excluding Sanriku part				
Hidaka (base)	40	17.87	1.0	8.72
Hidaka-1	32	14.29	0.8	8.65
Hidaka-2	24	10.72	0.6	8.57

The HEKT model shows the Hokkaido (2012) model, excluding the Kuril Trench part, and the Hidaka models show the Cabinet Office (2020) model (Sanriku-Hidaka model), excluding the Sanriku part. The fault slip factor is a multiplier for the slip amount in the original Sanriku-Hidaka model

*Rigidity is assumed to be 40 GPa

Table 4 Fault parameters of newly proposed models with 6, 10, 14, and 18 m slip amounts

Fault model		Depth (km)	Length (km)	Width (km)	Dip (°)	Strike (°)	Rake (°)	Slip (m)	Mw*
S	S1	5	150	100	11	215	90	6	8.30
	S1	5	150	100	11	215	90	10	8.45
	S1	5	150	100	11	215	90	14	8.55
	S1	5	150	100	11	215	90	18	8.62
	S2	24	150	100	21	215	90	6	8.30
	S2	24	150	100	21	215	90	10	8.45
	S2	24	150	100	21	215	90	14	8.55
	S2	24	150	100	21	215	90	18	8.62
T	T1	5	150	100	10	205	90	6	8.30
	T1	5	150	100	10	205	90	10	8.45
	T1	5	150	100	10	205	90	14	8.55
	T1	5	150	100	10	205	90	18	8.62
	T2	22	150	100	20	205	90	6	8.30
	T2	22	150	100	20	205	90	10	8.45
	T2	22	150	100	20	205	90	14	8.55
	T2	22	150	100	20	205	90	18	8.62
U	U1	5	150	100	9	195	90	6	8.30
	U1	5	150	100	9	195	90	10	8.45
	U1	5	150	100	9	195	90	14	8.55
	U1	5	150	100	9	195	90	18	8.62
	U2	21	150	100	17	195	90	6	8.30
	U2	21	150	100	17	195	90	10	8.45
	U2	21	150	100	17	195	90	14	8.55
	U2	21	150	100	17	195	90	18	8.62

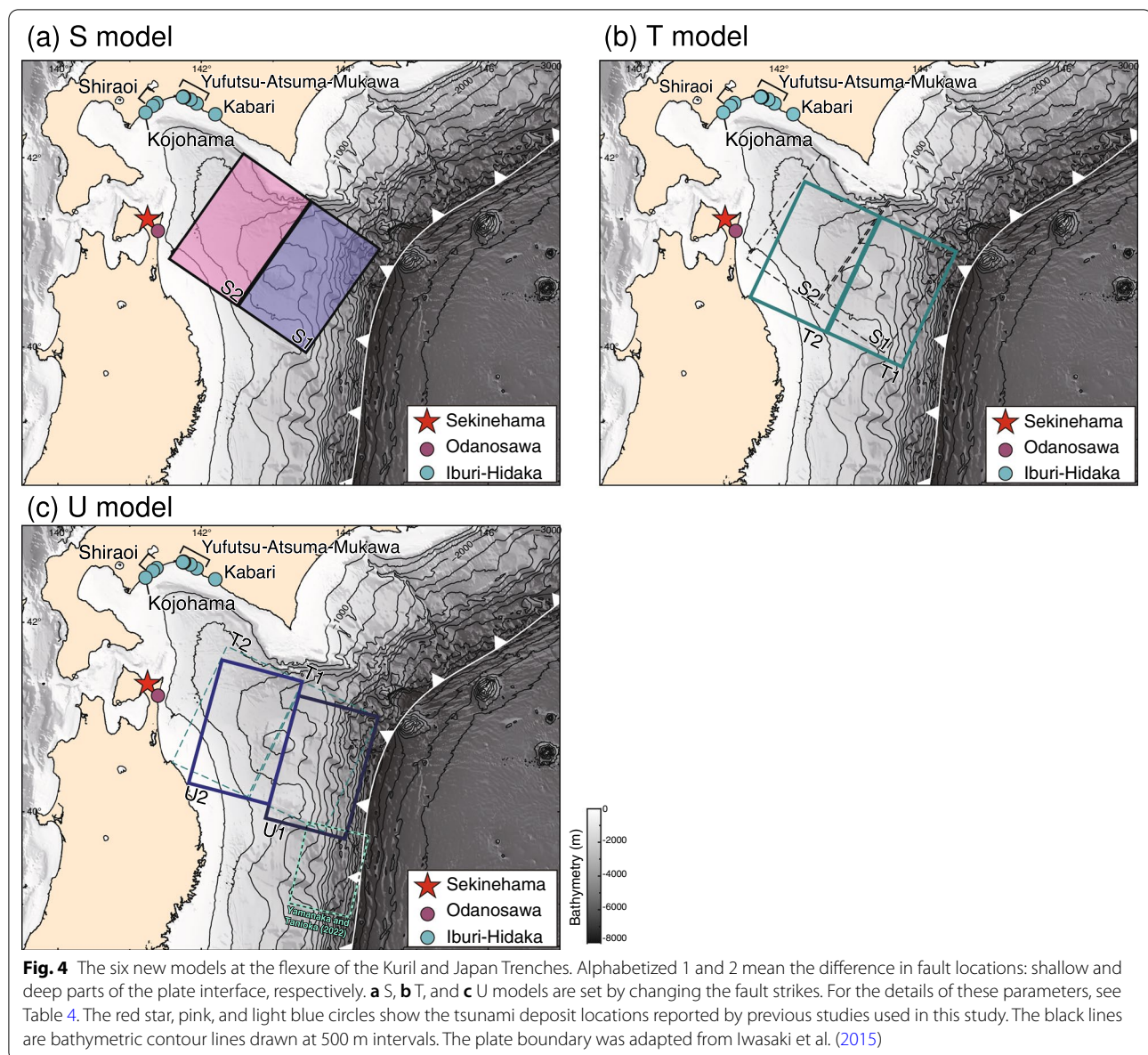
*Rigidity is assumed to be 40 GPa

the 1677 CE Empo tsunami is available. Regarding the tsunami related to submarine active fault movements, there is a wave-cut bench in the northwestern part of the Shimokita Peninsula. This is thought to be formed by twice-coseismic uplift events in the Holocene associated with the movement of the east–west oriented and south-dipping submarine reverse faults (Watanabe et al. 2012). The area of the northern Shimokita Peninsula has been uplifted 0.5–3 m by past single fault movement (Watanabe et al. 2012; Table 2).

Second, we examined the HEKT model, excluding the Kuril Trench part, from the Hokkaido (2012) model, and the Hidaka model, which cut Off the Sanriku part (Japan Trench part) from the Cabinet Office (2020) model (Sanriku-Hidaka model) (Table 3). We also examined four modification models (i.e., HEKT-1, HEKT-2, Hidaka-1, and Hidaka-2; Table 3) after reducing the slip amount of the two models, HEKT (base) and Hidaka (base) models. The three Hidaka models (i.e., Hidaka (base), Hidaka-1 and Hidaka-2) were simulated assuming the instantaneous fault rupture (60 s of rise time and rupture).

Finally, we assumed three fault models associated with an interplate earthquake at the flexural area between

Kuril and Japan Trenches with strike angles of 215° (S model), 205° (T model), and 195° (U model; parallel to northern Japan Trench) to illustrate the tsunami deposit distributions at Sekinehama and other sites (Fig. 4 and Table 4). Each model was divided into two fault ruptures—shallow part (S1, T1, and U1) and deep part (S2, T2, and U2)—yielding six models. For all these models, the fault length and width were fixed at 150 and 100 km, respectively. The fault origin coordinate (longitude and latitude) was the same for the T and U models, whereas the S model was translated slightly northeastward to cover the entire flexural area of the Kuril and Japan Trenches. The fault upper depth of S1, T1, and U1 (shallow part of plate interface) models was fixed at 5 km, and their fault dip was set at 11°, 10°, and 9°, respectively (Table 4). Conversely, the fault upper depth of S2, T2, and U2 (deep part of plate interface) models was set at 24 km, 22 km, and 21 km, and their fault dips were set at 21°, 20°, and 17°, respectively (Table 4). These fault plane parameters were assigned according to plate isobath data by Iwasaki et al. (2015) (Fig. 5). Except for the U model which is parallel to the Japan Trench, the lowermost depths of the S and T models, whose strikes are oriented

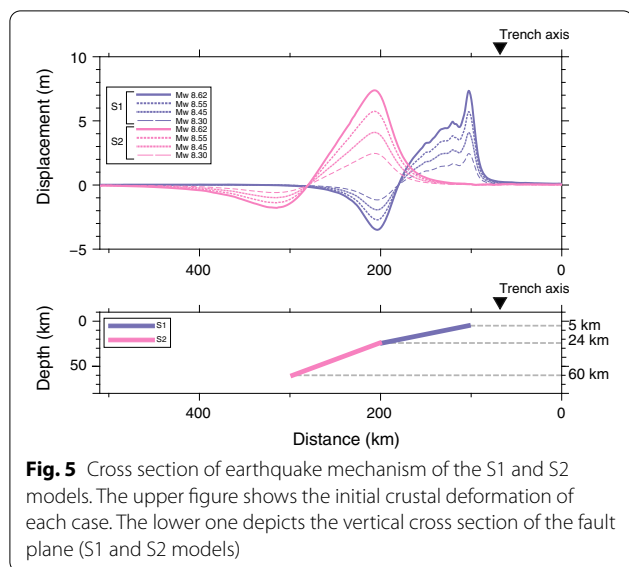


toward the Kuril Trench axis, were obtained by averaging the depths of the two western origin coordinates of the fault model from a plate isobath data and fitting the fault dip according to this value. A slip angle (rake) was 90° in common indicating a pure reverse fault earthquake. The slip amounts and associated moment magnitude of the models were charged as 6 m (Mw 8.30), 10 m (Mw 8.45), 14 m (Mw 8.55), and 18 m (Mw 8.62) (Table 4).

The initial computed tsunami height, vertical deformation from the seafloor, of the S models with 18 m slip was approximately 7.5 m (Fig. 5). The wavelength of the S1

model located at the shallow part of the plate interface is shorter than that of the S2 model (Fig. 5).

After the simulation by historical models, we examined the appropriate source and minimum tsunami size that can explain tsunami deposit distributions at Sekinehama and Odanosawa along the coasts of the Shimokita Peninsula (Fig. 1a and b) using the six modified previously described models and six new fault models. Then, they were also examined at the other sites along the Iburi-Hidaka coast in southwestern Hokkaido using the models with the appropriate fault parameters to ascertain



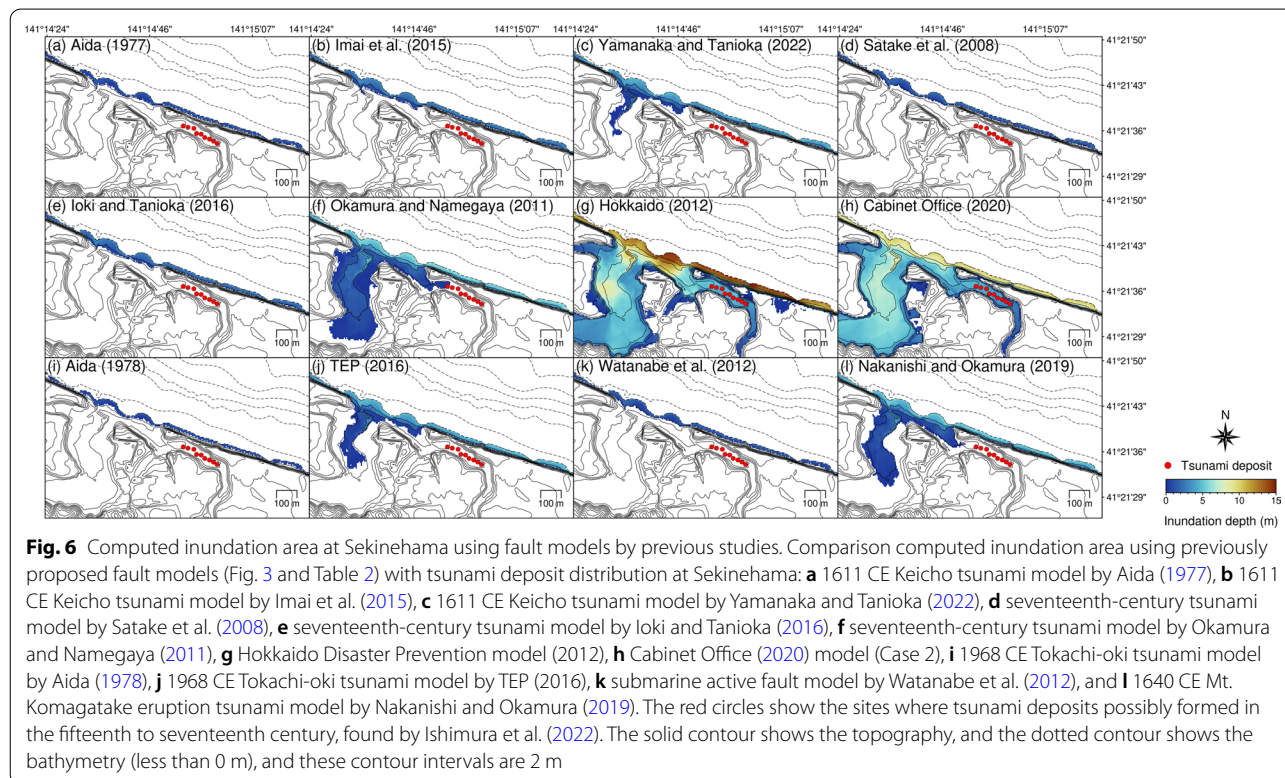
whether the tsunami deposits there can be explained by the models. The appropriate models were determined according to the calculated inundation depth at the most inland location where the tsunami deposit distributions in the fifteenth to seventeenth century at Sekinehama (SKN-GS2) and in the fifteenth to eighteenth century at Odanosawa (N5&6, hereafter called N6) on the coast of Shimokita Peninsula were observed.

4 Computational results and interpretations

4.1 Calculated inundation area at Sekinehama with the previous models

4.1.1 The 1611 CE Keicho and seventeenth-century tsunami models

The three 1611 CE Keicho tsunami models (Aida 1977; Imai et al. 2015; Yamanaka and Tanioka 2022) and three seventeenth-century tsunami models (Satake et al. 2008; Okamura and Namegaya 2011; Ioki and Tanioka 2016) resulted in a small inundation and could not explain the tsunami deposit distribution at Sekinehama (Fig. 6a–f). The inundation area and maximum run-up height from Aida (1977) model along the Japan Trench were smaller than those from the models by Ioki and Tanioka (2016) and Satake et al. (2008) along the Kuril Trench (Fig. 6a, d, and e). The calculation result from Imai et al. (2015) model with Mw 8.7 (maximum setting) was similar to that of Ioki and Tanioka (2016) model (Mw 8.8) (Fig. 6b and e). Yamanaka and Tanioka (2022) model, which is the latest 1611 CE Keicho tsunami model (Mw 8.5), yielded a larger inundation than the models described above, but could not explain the tsunami deposit distribution as well (Fig. 6c). Okamura and Namegaya (2011) model (Mw 8.9) along the Kuril Trench is set in the same segment as the T10N5 model (Satake et al. 2008) but has three times the slip amount. It resulted in a higher



inundation area and run-up height than Ioki and Tanioka (2016) model but did not reach the far end of the tsunami deposit distribution (Fig. 6f), implying that only a large fault rupture in Kuril (> Mw 8.8) or Japan (> Mw 8.3–8.7) Trenches alone could not explain the tsunami deposit distribution. The Hokkaido (2012) (Mw 9.2) and Cabinet Office (2020) models (Case 2 of the Sanriku-Hidaka model; Mw 9.1) produced large inundations and were appropriate models that could account for the most inland tsunami deposit (Fig. 6g and h).

4.1.2 Other models

The computed inundation area and maximum run-up height of the 1968 CE Tokachi-oki tsunami model (in substitution for the 1677 CE Empo tsunami; Aida 1978) and submarine active fault model (Watanabe et al. 2012) were similar to those of the 1611 CE Keicho tsunami model (Mw 8.3) proposed by Aida (1977) (Fig. 6i and k). They could not explain the tsunami deposit distribution. The computed inundation area of the 1968 CE Tokachi-oki tsunami model by TEP (2016) could not explain it but produced a slightly larger inundation and maximum run-up height than in the 1611 CE Keicho tsunami model, despite its smaller rupture area (Figs. 3a and 6j). The computed result of the maximum tsunami model associated with the 1640 CE Mt. Komagatake eruption, which is proposed by Nakanishi and Okamura (2019), was slightly larger than that of the TEP (2016) model and could not explain the tsunami deposits (Fig. 6l). In summary here, the calculated inundation area using the models described in this section could not satisfy the tsunami deposit distribution at Sekinehama.

4.2 Computed inundation area at Odanosawa with the previous models

The Hokkaido (2012) (Mw 9.2) and Cabinet Office (2020) models (Mw 9.1) (Fig. 3b and Table 2) could explain the most inland tsunami deposit found more than 1 km inland (site N6; Tanigawa et al. 2014) (Additional file 2:

Fig. S1g and h), whereas the other models could not explain even the seaward-most tsunami deposit (Additional file 2: Fig. S1a–f, i–l). These results were similar to those of Sekinehama, implying that the tsunami deposits on the north and east coasts of the Shimokita Peninsula are explained by only fault models that include the rupture at the flexural area of the Kuril and Japan Trenches.

4.3 Computed inundation area with the modified previously described models

Based on the computer simulation results of previously proposed models, the large interplate earthquake along Kuril or Japan Trenches alone could not satisfy the tsunami deposit distributions at Sekinehama and Odanosawa on the coast of the Shimokita Peninsula, thereby implying that the fault rupture at the flexural area of the two trenches is necessary to explain them. Hence, we examined the modified previously described models to explain the above-mentioned tsunami deposits and those preserved on the Iburi–Hidaka coast, the PC of southwestern Hokkaido (Fig. 1c–f), and to evaluate the tsunami source and minimum size of the large earthquake on the bend area of the two trenches.

4.3.1 Sekinehama and Odanosawa

The two modification models, HEKT (base) and Hidaka (base) models (Fig. 3b and Table 3), could explain tsunami deposits at two sites, Sekinehama and Odanosawa, on the north and east coasts of the Shimokita Peninsula (Table 5). The HEKT-1 and Hidaka-1 models reducing slip amounts from the original ones could also account for tsunami deposit distributions at the two sites (Table 5). However, the HEKT-2 and Hidaka-2 models could not explain them at the two sites. Therefore, the minimum tsunami size that could explain tsunami deposit distributions at Sekinehama and Odanosawa, using modified previous proposed models, were Mw 8.76 (HEKT-1), whose slip has 25 m (shallow part) and 20 m (deep part), and Mw 8.65 (Hidaka-1), whose average slip has 14.29 m (Tables 3 and 5). The average slip amount of

Table 5 Computed inundation depth at Sekinehama and Odanosawa using the modified previously proposed models

Site	Fault model					
	HEKT model: Hokkaido (2012) model excluding Kuril Trench part			Hidaka model: Cabinet Office (2020) model excluding Sanriku part		
	HEKT (base)	HEKT-1	HEKT-2	Hidaka (base)	Hidaka-1	Hidaka-2
Sekinehama-GS2	4.9	2.9	0.2	4.5	2.7	–
Odanosawa-N6	4.0	0.8	–	6.4	3.0	–
Mw	8.87	8.76	8.59	8.72	8.65	8.57

The inundation depth was computed at Sekinehama-GS2, which is the most inland tsunami deposit identified by Ishimura et al. (2022), and at Odanosawa-N6, which is the most inland tsunami deposit identified by Tanigawa et al. (2014). The bold number shows that the most inland tsunami deposits at the two sites could be explained simultaneously

the former model needs larger values (22.5 m) than that of the latter model partly because its strike (225°) is similar to the average strike (228°) of the Kuril Trench axis (Fig. 3b).

4.3.2 Iburi–Hidaka coast

The tsunami deposit distributions along the Iburi–Hidaka coast (Fig. 1c–e) were compared with the calculated inundation areas by the above-mentioned four fault models, HEKT (base), HEKT-1, Hidaka (base), and Hidaka-1 models, which could explain the most inland tsunami deposit at Sekinehama and Odanosawa simultaneously. Only the Hidaka (base) model could explain tsunami deposit distributions on the Iburi–Hidaka coast in southwestern Hokkaido, same as the Cabinet Office (2020) model. The other three models, HEKT (base), HEKT-1, and Hidaka-1 models, could not sufficiently explain tsunami deposit distributions on the Iburi–Hidaka coast simultaneously. In the case of HEKT models, it is clear that a fault rupture in the Kuril Trench part is needed to explain tsunami deposits on the Iburi–Hidaka coast as in the Hokkaido (2012) model.

4.4 Computed inundation area with the newly proposed models

Tsunami simulations using modified previously proposed models revealed that the large fault rupture at the flexural area of the Kuril and Japan Trenches helped explain the tsunami deposit distributions on the coast of the Shimokita Peninsula. However, we could not sufficiently discuss the tsunami sources and minimum sizes that can explain the tsunami deposit data used in this study because the fault parameters of the Hidaka and the HEKT models considered in the previous chapter varied from each other (e.g., fault geometry, strike, etc.). With the fault model covering the flexural area of the two trenches and

fixing some parameters, we newly examined the tsunami source and minimum size that can most critically account for the tsunami deposits.

4.4.1 Sekinehama and Odanosawa

We examined six new fault models that cover the flexural area of the Kuril and Japan Trenches from the shallow to deep parts of the plate interface (Fig. 4). We calculated the tsunami inundation areas at two sites using the S1, S2, T1, T2, U1, and U2 models. We calculated a total of 24 cases using the six new models placed at the flexure of the Kuril and Japan Trenches (Table 4). For each of the S1, S2, T1, T2, U1, and U2 models, four patterns of slip amount (6, 10, 14, and 18 m) at the shallow part (S1, T1, and U1) and deep part (S2, T2, and U2) of the plate interface were calculated (Fig. 4 and Table 4). These models, except for U1, could satisfy the tsunami deposit distributions at the two sites when the slip amount was 18 m (Table 6). The most inland tsunami deposits at the two sites could be explained by the S1, S2, and T2 models with 14 m slip, whereas the other models with 14, 10, and 6 m slip could not explain them (Table 6). The deep rupture models (S2, T2, and U2 models) tended to be more inundated on the two sites than the shallow rupture ones (S1, T1, and U1 models). For the U model, a large fault slip (18 m) in the deep plate interface (U2 model) is needed to explain the most inland tsunami deposit at the two sites by an identical event.

Therefore, the S1, S2, and T2 models with a 14 or 18 m slip and the T1 and U2 models with an 18 m slip were appropriate to explain the tsunami deposit distributions at Sekinehama and Odanosawa simultaneously (Table 6). In addition, S and T models could better explain the tsunami deposit distributions at the two sites than the U model (Table 6). These results probably depend on the strike, implying that the fault models slightly tilted

Table 6 Computed inundation depth at Sekinehama and Odanosawa using six newly proposed fault models

Site	Shallow rupture model			Deep rupture model			Slip (m)
	S1	T1	U1	S2	T2	U2	
Sekinehama-GS2	–	–	–	–	–	–	6
Odanosawa-N6	–	–	–	–	–	–	
Sekinehama-GS2	–	–	–	–	–	–	10
Odanosawa-N6	–	–	–	–	0.5	–	
Sekinehama-GS2	0.6	–	–	0.9	0.4	–	14
Odanosawa-N6	0.5	–	–	3.3	5.2	4.3	
Sekinehama-GS2	3.1	1.1	–	3.6	3.1	2.0	18
Odanosawa-N6	4.0	2.6	0.7	7.2	8.9	8.0	

The inundation depth was computed at Sekinehama-GS2, which is the most inland tsunami deposit identified by Ishimura et al. (2022), and at Odanosawa-N6, which is the most inland tsunami deposit identified by Tanigawa et al. (2014). The bold number depicts that the most inland tsunami deposits at the two sites could be explained simultaneously

toward the Kuril Trench (S and T models; strike of 205° and 215°) were more suitable than those parallel to the northern Japan Trench (U model; strike of 195°) (Fig. 7).

4.4.2 Iburi–Hidaka coast

Based on the results mentioned in the previous chapter, we employed six fault models (S1, S2, and T2 models

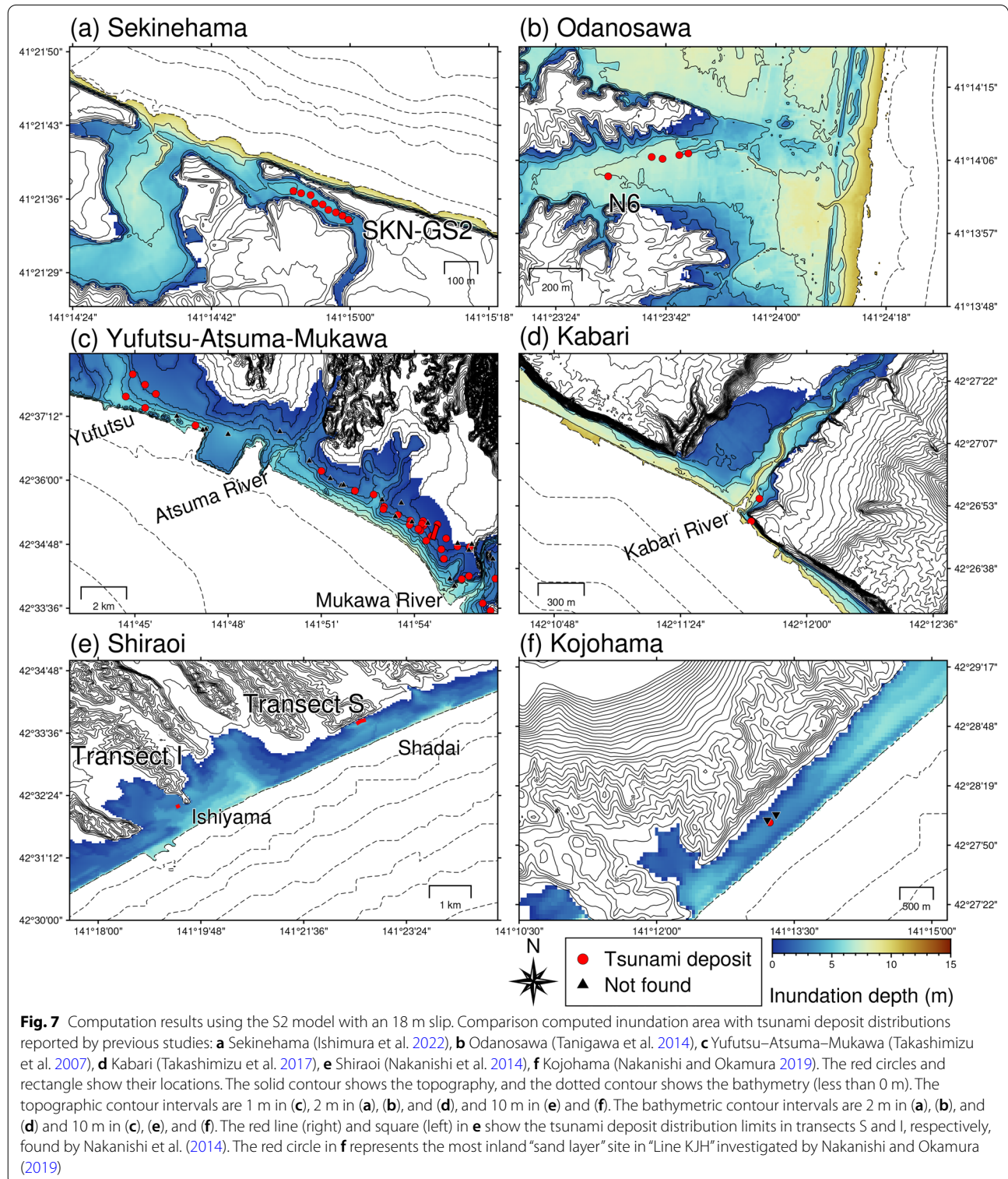


Fig. 7 Computation results using the S2 model with an 18 m slip. Comparison computed inundation area with tsunami deposit distributions reported by previous studies: **a** Sekinehama (Ishimura et al. 2022), **b** Odanosawa (Tanigawa et al. 2014), **c** Yufutsu–Atsuma–Mukawa (Takashimizu et al. 2007), **d** Kabari (Takashimizu et al. 2017), **e** Shiraoui (Nakanishi et al. 2014), **f** Kojohama (Nakanishi and Okamura 2019). The red circles and rectangle show their locations. The solid contour shows the topography, and the dotted contour shows the bathymetry (less than 0 m). The topographic contour intervals are 1 m in (c), 2 m in (a), (b), and (d), and 10 m in (e) and (f). The bathymetric contour intervals are 2 m in (a), (b), and (d) and 10 m in (c), (e), and (f). The red line (right) and square (left) in **e** show the tsunami deposit distribution limits in transects S and I, respectively, found by Nakanishi et al. (2014). The red circle in **f** represents the most inland “sand layer” site in “Line KJH” investigated by Nakanishi and Okamura (2019)

with a 14 m or 18 m slip) and two fault models (T1 and U2 models with an 18 m slip) to evaluate the calculated inundation area at the other sites along the Iburi–Hidaka coast. The tsunami deposit distributions along the Iburi–Hidaka coast were compared with the calculated inundation areas by the above-mentioned eight fault models that could explain the most inland tsunami deposit at Sekinehama and Odanosawa simultaneously. The S2 model with an 18 m slip was the only model that could explain tsunami deposit distributions at all sites simultaneously (Sekinehama and Odanosawa along the coast of Shimokita Peninsula and Yufutsu–Atsuma–Mukawa, Kabari, Shiraoui, and Kojohama along the Iburi–Hidaka coast in southwestern Hokkaido; Figs. 7 and 8).

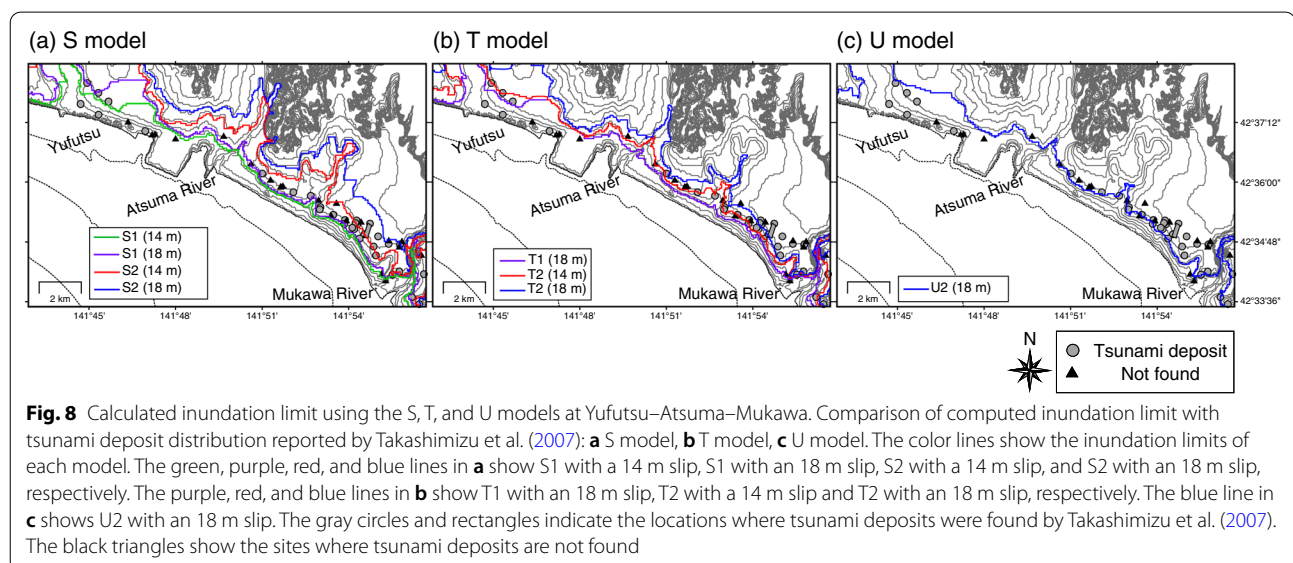
The computation results using the S1, S2, and T2 models with a 14 m slip as well as the S1, T1, T2, and U2 models with an 18 m slip could not explain the tsunami deposit distributions at the Yufutsu–Atsuma–Mukawa coast (Fig. 1c; Takashimizu et al. 2007) on the eastern Iburi coast (Fig. 8a–c). The S2 model with an 18 m slip yielded the largest inundation (Figs. 7c and 8a), and it was the most appropriate model that could account for tsunami deposit distribution along the eastern Iburi coast. The calculated tsunami inundation using the S2 model with a 14 m slip could cover tsunami deposit distributions at the Yufutsu and Atsuma Rivers but not around the Mukawa River (Fig. 8a). Moreover, the tsunami deposits in the coastal outcrop near the Kabari River on the western Hidaka coast (Fig. 1d; Takashimizu et al. 2017) could be explained by eight fault models that could explain tsunami deposits at Sekinehama and Odanosawa (Fig. 7d and Additional file 3: Fig. S2a–g).

The computation results of the newly proposed models were also evaluated at Shadaei and Ishiyama in Shiraoui (Fig. 1e; Nakanishi et al. 2014). The S2 model with a 14 and 18 m slip and the T2 model with an 18 m slip could explain the tsunami deposit distributions along transects S and I at Shiraoui (Fig. 7e and Additional file 4: Fig. S3c, f). This result agrees with the suggestion following the geological investigation by Nakanishi et al. (2014) that the tsunami deposits in Shiraoui were explained by a tsunami associated with the Hokkaido (2012) model located in the flexural area of Kuril and Japan Trenches. Further, the tsunami deposit distribution at Kojohama (Fig. 1f; Nakanishi and Okamura 2019) along the western Iburi coast was also explained by these models (Fig. 7f and Additional file 5: Fig. S4c, f). The other models could not explain the most inland tsunami deposit in Shiraoui and Kojohama (Additional file 4: Fig. S3 and Additional file 5: Fig. S4).

5 Discussion

5.1 Summary of fault models that could explain tsunami deposit distributions and minimum tsunami size

The computational results showed that two previously proposed and four modified models (i.e., Hokkaido (2012), Cabinet Office (2020), HEKT (base), HEKT-1, Hidaka (base), and Hidaka-1 models; 20–40 m slip) and eight newly proposed models (S1, S2, T2 models with a 14 m or 18 m slip, T2 and U2 models with an 18 m slip), whose sources are placed at the flexural area of Kuril and Japan Trenches, could explain tsunami deposit distributions at Sekinehama and Odanosawa on the coast of Shimokita Peninsula (Tables 5–6). According to the previous studies and our numerical simulations, the



Hokkaido (2012), Cabinet Office (2020), Hidaka (base), and S2 (18 m slip) models (18–40 m slip) could also explain tsunami deposit distributions along the Iburī–Hidaka coast in southwestern Hokkaido. The amount of slip using new fault models in the deep plate boundary (S2, T2, and U2; 14–18 m) is coherent with those using the Hidaka (base) and Hidaka-1 models (avg. 14.29–17.87 m), whose sources are located at the deep plate boundary. By contrast, the slip amount of the HEKT and HEKT-1 models (20–35 m) is large compared to that of the new fault model in the shallow plate boundary (S1; 14–18 m). One of the reasons for this may be that the strike (225°) of the former is oriented to the Kuril Trench axis (Fig. 3b). These computation results imply that when a large interplate earthquake occurs somewhere in the flexural area, there should be at least 14–40 m of slip to fully explain tsunami deposits around the seventeenth century on the PC of northern Japan.

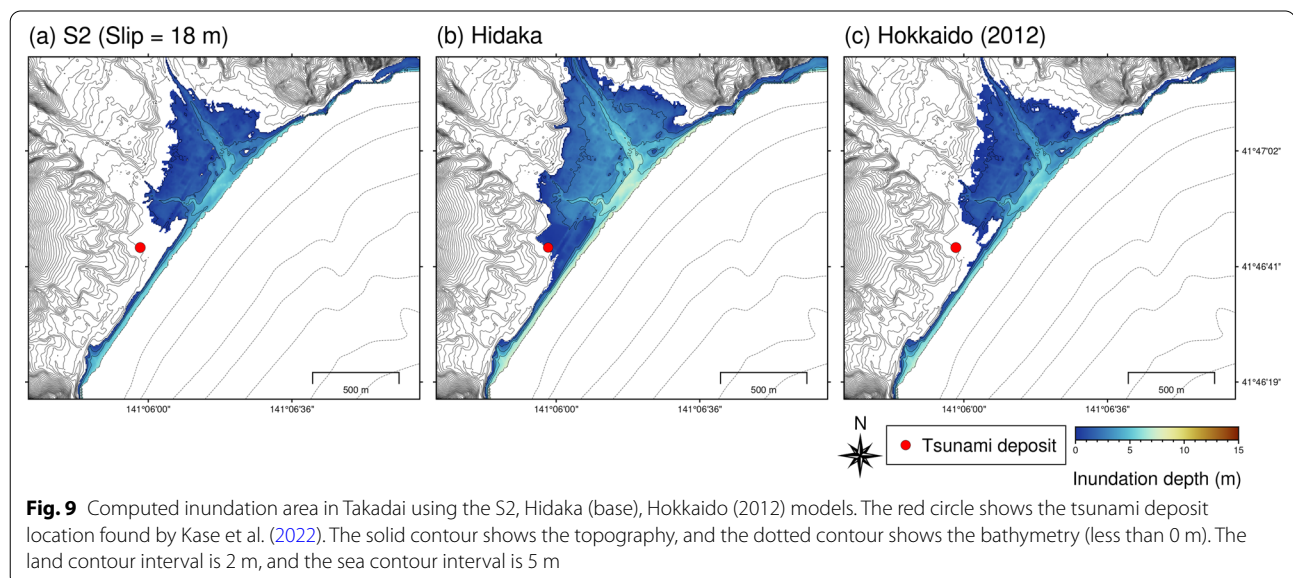
The minimum tsunami size that explains the tsunami deposits on the coast of the Shimokita Peninsula was found to be Mw 8.55 (S1, S2, T2 models; 14 m slip); when these deposits along the Iburī–Hidaka coast in southwestern Hokkaido were to be explained by the same event, the minimum tsunami size was found to be Mw 8.62 (S2 model; 18 m slip). In subsequent sections, we examine the adequacy of the three models, S2 (18 m slip), Hidaka (base; avg. 17.87 m slip), and Hokkaido (2012) models, because they are appropriate models in this study that could sufficiently explain tsunami deposit distributions possibly formed around the seventeenth century from the southwestern Hokkaido to the north and east coasts of Shimokita Peninsula.

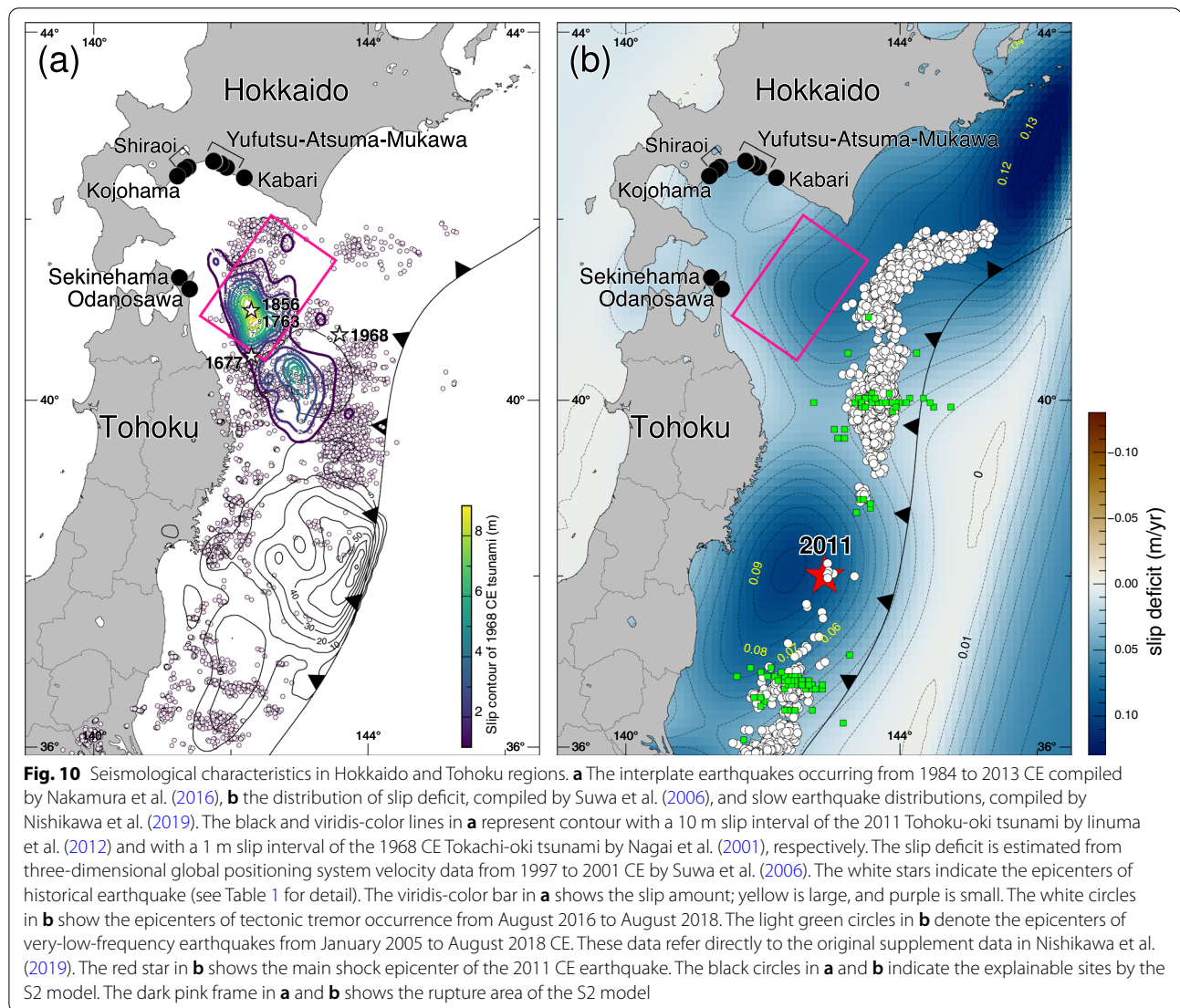
5.2 Evaluation of three fault models using the tsunami deposit at Takadai in southwestern Hokkaido

According to a geological study performed by Kase et al. (2022), large tsunamis around the seventeenth century had little or no influence in Takadai on the PC of southern Hokkaido (Figs. 1j and 2) because there were no tsunami deposits around the seventeenth century. In this study, the Hokkaido (2012), Hidaka (base), and S2 models did not reach the studied location in Takadai (Fig. 9a–c). Moreover, the S2 model resulted in the smallest inundation area among the three models. Even though the Hidaka (base) and S2 models show similar rupture zones, the former has a larger inundation area than the latter because the former's rupture zone and initial water level distribution are located nearer to the continental side than those of the latter. In contrast, the fault area of the Hokkaido (2012) model exists far from Takadai, near the trench axis. However, the inundation area of the Hokkaido (2012) model is larger than that of the S2 model because the average slip amount is approximately twice. Hence, the tsunami impact at Takadai in the seventeenth century is estimated to be smaller when the rupture zone is located at the deep part of the plate interface, as in the S2 model.

5.3 Seismological validity of the interplate earthquake models discussed in this study

Past interplate earthquakes about three decades have occurred not only Off Sanriku and Miyagi but also Off Aomori in which the rupture zone of the Hidaka (base) and S2 models is located (Fig. 10a). The S2 model (18 m slip) fault rupture depths from 24 to 60 km and its spatial extent roughly correspond to the locations where the past





interplate earthquakes could have occurred (Fig. 10a); thus, it is not inconsistent that there would have been ruptures in these locations during the fifteenth to seventeenth century. The unusually large fault slip of the 2011 Tohoku-oki tsunami (Mw 9.0) occurred in asperities facing the central part of the Japan Trench, whereas the 1968 CE Tokachi-oki tsunami (M 7.9) occurred in asperities facing the north part of the Japan Trench (Fig. 10a). The southwest side of the S2 or Hidaka (base) models coincides with the northern part of the latter asperity in the northern Japan Trench, whereas the northeast side is thought to be a blank area of past interplate earthquakes (Fig. 10a). Hence, the spatial rupture area of the S2 or Hidaka (base) models has a high potential to have witnessed large earthquakes.

Suwa et al. (2006) estimated the plate coupling in northeastern Japan using a geodetic inversion of

three-dimensional global positioning system (3D GPS) velocity data during 1997–2001 CE. According to this analysis, the slip deficit in northern Japan is about 6–7 cm/yr in the S2 or Hidaka (base) model rupture zones (Fig. 10b). This zone's plate coupling rate is stronger than that near the northern Japan Trench axis, the rupture zone of the S1, U1, and HEKT models, implying that a large earthquake (>M 8) like the 1968 CE Tokachi-oki tsunami (M 7.9) had also possibly occurred there in the past fifteenth to seventeenth century because the rupture area in the deep plate boundary of the S2 or Hidaka (base) models accumulates strain more easily than in the near trench axis (Fig. 10b).

Slow earthquakes are classified as tectonic tremors, very low-frequency earthquakes (VLFs), and slow-slip events, and their occurrences have been reported to be closely related to that of large earthquakes (e.g.,

Obara and Kato 2016; Nishikawa et al. 2019). The 2011 CE Tohoku-oki earthquake was estimated to have been caused by the rupture propagating from the central part of the Japan Trench and stopped in the slow earthquake zone north and south of these rupture areas (Nishikawa et al. 2019). Moreover, a detailed slow earthquake map from 1991 to 2018 CE along the Japan Trench suggests that the areas where large interplate and slow earthquakes occurred are segregated from each other (Nishikawa et al. 2019). The rupture zones of the 2011 CE Tohoku-oki earthquake coincide with plate consolidation extents where slow earthquakes are unlikely to occur, and the rupture zone of the S2 and Hidaka (base) models is similar to them (Fig. 10b). Therefore, the geodetic data based on these recent seismological observations imply that the S2 and Hidaka (base) models are placed at a location where large earthquakes of more than $>M 8$ possibly occur. The rupture zone of the shallow part of the plate interface near the trench axis (i.e., HEKT (base) and Hokkaido (2012) models) almost covers the area where slow earthquake events occurred (Fig. 10b).

5.4 Implications for large tsunamis in the fifteenth to seventeenth century

This chapter discusses the implications of the computed inundation area using the fault models considered in this study for the PC of Tohoku and Hokkaido. First, we compared the computed inundation area using the S2, Hidaka (base), and Hokkaido (2012) models with the tsunami deposit distribution formed in the seventeenth century in the eastern PC of Hokkaido (Fig. 1g; Nanayama et al. 2002). The S2 (18 m slip) and Hidaka (base; avg. 17.87 m slip) models resulted in a smaller inundation area than the tsunami deposit distribution at Oikamanai, a coastal pond in the eastern PC of Hokkaido, facing the Kuril Trench (Additional file 6: Fig. S5a and Additional file 7: Fig. S6a). The tsunami deposit distribution at Oikamanai pond in the eastern PC of Hokkaido can be traced to more than 4 km from the present shoreline (Fig. 1g; Nanayama et al. 2002). Therefore, there is a high probability that the S2 and Hidaka (base) models could not account for tsunami deposits in the coastal area of the Tokachi coasts in the eastern PC of Hokkaido.

At the Mochirippu swamp on the eastern Nemuro coast, diatom analysis reveals that pre-seismic subsidence and post-seismic uplift associated with an interplate earthquake in the seventeenth century are recorded in the mud and peat sequence preserved in a pond (Sawai et al. 2004). Thus, the unusual interplate earthquake such as the T10N5S25 model (Ioki and Tanioka 2016; $>Mw 8.8$) is needed to satisfy the above-mentioned geological records on the eastern PC of Hokkaido because the S2 (18 m slip) and Hidaka (base) models could not recover

pre-seismic subsidence in the eastern PC of Hokkaido. Moreover, no event deposits have been identified in or near the same stratigraphic level as the seventeenth-century tsunami deposit in the drilled core on the area of the Tokachi to Nemuro coasts in the eastern PC of Hokkaido. Therefore, there is a high probability that even if a tsunami related to a large earthquake occurred in the flexure of the Kuril and Japan Trenches, such as the S2 and Hidaka (base) models, it could not be preserved as a geological record along the Tokachi to Nemuro coasts. In contrast, the Hokkaido (2012) model could explain the tsunami deposit at Oikamanai pond because it has a large slip (30–35 m) along the wide area of the Kuril Trench (Hokkaido 2012).

Second, using the S2 (18 m slip), Hidaka (base), and Hokkaido (2012) models, we compared the computed inundation area with the tsunami deposit distributions possibly formed by the 1611 CE Keicho tsunami on the Sanriku coast. The S2 (18 m slip) and Hidaka (base; avg. 17.87 m slip) models resulted in a smaller inundation area than the tsunami deposit distributions at the two sites, Harashinai and Masaki on the Sanriku coast facing the Japan Trench. (Additional file 6: Fig. S5b, c and Additional file 7: Fig. S6b, c).

Tsunami deposits formed by the 1611 CE Keicho tsunami have been reported along the Sanriku coast facing the Japan Trench (e.g., Goto et al. 2015, 2019; Takada et al. 2016; Ishizawa et al. 2022). Among these, the northernmost tsunami deposit estimated to have been formed by the 1611 CE Keicho tsunami is preserved at Harashinai in northern Iwate (Fig. 1h; Takada et al. 2016). According to the tsunami simulation results, it may be presumed that the tsunami source that can explain the tsunami deposits of the 1611 CE Keicho tsunami needs a rupture zone Off Sanriku on the central to the northern parts of the Japan Trench such as the U and Cabinet Office (2020) models. On the contrary, the Hokkaido (2012) model could explain the tsunami deposits at Harashinai and Masaki because of the large slip (30–35 m) in the junction area of Kuril and Japan Trenches.

Therefore, by comparing the calculated inundation with the tsunami deposit distributions along the PC of southwestern Hokkaido and the Shimokita Peninsula, the computation results elucidated the possibility that an interplate earthquake with a large slip (>14 – 40 m slip) occurred at the flexure of the Kuril and Japan Trenches in the fifteenth to seventeenth century. Tetsuka et al. (2020) mentioned the possibility that large tsunamis (i.e., 1611 CE Keicho tsunami or seventeenth-century tsunami, etc.) occurred one huge or two to three large tsunamis from the Kuril to Japan Trenches around the seventeenth century. Our results suggest that an interplate earthquake of more than $M 8$ occurred at the junction of the Kuril and

Japan Trenches in the fifteenth to seventeenth century and support the occurrence of multiple large earthquakes in the Kuril and Japan Trenches with short intervals.

6 Conclusions

To estimate a tsunami source that can explain the 1450–1650 CE (fifteenth to seventeenth century) tsunami deposit distribution at Sekinehama on the north coast of Shimokita Peninsula, we first performed numerical simulations using the previously reported fault models of the 1611 CE Keicho tsunami along Japan Trench ($>M_w$ 8.3–8.7), the seventeenth-century tsunami along the Kuril Trench ($>M_w$ 8.8), and other possible tsunami sources (the 1677 CE Empo tsunami, a tsunami associated with the 1640 CE Komagatake volcanic eruption, a submarine active fault, and the disaster prevention model). However, these models could not explain the tsunami deposits showing similar ages at Sekinehama and another site on the coast of Shimokita Peninsula, which are within 50 km apart, except with the two huge earthquake models ($>M_w$ 9.1; the disaster prevention models). The rupture areas of these two models extend to the Kuril or Japan Trenches and their flexural area. We then examined six modified previously described fault models and six newly proposed fault models in the flexural area of the Kuril and Japan Trenches to explain the tsunami deposit distributions possibly formed around the seventeenth century at the above-mentioned two sites on the coast of the Shimokita Peninsula. The appropriate tsunami source and its minimum tsunami size are examined by changing fault parameters. The result of the numerical analysis shows that a more than 14–32 m slip ($>M_w$ 8.55–8.76) on the shallow or deep parts of the plate interface is required. When the above tsunami deposits together with those formed around the seventeenth century along the Iburī–Hidaka coast in southwestern Hokkaido were left by the same event, more than 18–40 m slip ($>M_w$ 8.62–9.2) is needed on the plate interface at the flexure zone of the Kuril and Japan Trenches. According to recent slip deficit and slow earthquake data, it is possible that a large interplate earthquake on the deep part of the plate boundary occurred in the fifteenth to seventeenth century.

This work shows the 14–32 m slip at least along the plate interface in the flexural area of the Kuril and Japan Trenches in the fifteenth to seventeenth century. This result and previous studies indicate that in the fifteenth to seventeenth century, large interplate earthquakes of more than M 8.5, with a large slip amount of over 14 m, continuously occurred along the wide area of plate interface Off northern Japan, suggesting that the strain energy accumulated along that plate interface might be completely released in the fifteenth to seventeenth century.

This event may be associated with historical large earthquakes ($>M$ 8) in the Kuril and Japan Trenches, such as the seventeenth-century earthquake tsunami and the 1611 CE Keicho tsunami, or it may represent a completely unknown interplate earthquake that occurred at the flexural area of both trenches. For future work, paleotsunami investigations along the coastal area of the Hokkaido to Tohoku regions facing the Kuril and Japan Trench junction, geophysical observation, modeling, and careful evaluations of the historical record, including the 1611 CE Keicho tsunami (e.g., tsunami arrival time from maximum ground shaking), should be considered.

Abbreviations

Hokkaido (2012): Hokkaido Disaster Prevention Council (2012); TEP (2016): Tohoku Electric Power (2016).

Supplementary Information

The online version contains supplementary material available at <https://doi.org/10.1186/s40645-022-00530-2>.

Additional file 1: Table S1 The bathymetric data and tsunami deposit distribution data used in this study. The tsunami deposit distributions used in this study are noted with the original names of the corresponding reference studies.

Additional file 2: Fig. S1 Computed inundation area at Odanosawa using fault models by previous studies. Comparison computed inundation area using previously proposed fault models (Fig. 3 and Table 2) with tsunami deposit distribution at Sekinehama: **a** 1611 CE Keicho tsunami model by Aida (1977), **b** 1611 CE Keicho tsunami model by Imai et al. (2015), **c** 1611 CE Keicho tsunami model by Yamanaka and Tanioka (2022), **d** seventeenth century tsunami model by Satake et al. (2008), **e** seventeenth century tsunami model by Ioki and Tanioka (2016), **f** seventeenth century tsunami model by Okamura and Namegaya (2011), **g** Hokkaido Disaster Prevention model (2012), **h** Cabinet Office (2020) model (Case2), **i** 1968 CE Tokachi-oki tsunami model by Aida (1978), **j** 1968 CE Tokachi-oki tsunami model by TEP (2016), **k** submarine active fault model by Watanabe et al. (2012), and **l** 1640 CE Mt. Komagatake tsunami model by Nakanishi and Okamura (2019). The red circles show the sites where tsunami deposits possibly formed in the fifteenth to eighteenth century found by Tanigawa et al. (2014). The solid contour shows the topography. The dotted contour depicts the bathymetry (less than 0 m). The contour intervals are 2 m

Additional file 3: Fig. S2 Computation results using the S1, S2, T1, T2, and U2 models at Kabari. Comparison computed inundation area with tsunami deposit distributions reported by Takashimizu et al. (2007): **a** S1 model with M_w 8.55, **b** S1 model with M_w 8.62, **c** S2 model with M_w 8.55, **d** T1 model with M_w 8.62, **e** T2 model with M_w 8.55, **f** T2 model with M_w 8.62, **g** U2 model with M_w 8.62. The red circles show the tsunami deposit site found by Takashimizu et al. (2017)

Additional file 4: Fig. S3 Computation results using the S1, S2, T1, T2, and U2 models at Shirai. Comparison computed inundation area with tsunami deposit distributions reported by Takashimizu et al. (2007): **a** S1 model with M_w 8.55, **b** S1 model with M_w 8.62, **c** S2 model with M_w 8.55, **d** T1 model with M_w 8.62, **e** T2 model with M_w 8.55, **f** T2 model with M_w 8.62, **g** U2 model with M_w 8.62. The red line (right) and square (left) show the tsunami deposit distribution limits in transects S and I, respectively, found by Nakanishi et al. (2014)

Additional file 5: Fig. S4 (Computation results using the S1, S2, T1, T2, and U2 models at Kojohama. Comparison computed inundation area with tsunami deposit distributions reported by Nakanishi and Okamura (2019): **a** S1 model with M_w 8.55, **b** S1 model with M_w 8.62, **c** S2 model with M_w 8.55, **d** T1 model with M_w 8.62, **e** T2 model with M_w 8.55, **f** T2 model with

Mw 8.62, **g** U2 model with Mw 8.62. The red circle and black triangle show the tsunami and non-tsunami deposit sites, respectively, by Nakanishi and Okamura (2019). The red circle in **f** represents the most inland “sand layer” site in “Line KJH” investigated by Nakanishi and Okamura (2019)

Additional file 6: Fig. S5 Computed results using the S2 model at Oikamanai, Harashinai, and Masaki. The red circles show tsunami deposit locations **a** found by Nanayama et al. (2002) in Oikamanai pond and **b** and **c** found by Takada et al. (2016) in Harashinai and Masaki, respectively. The solid contour shows the topography, and the dotted contour shows the bathymetry (less than 0 m). The contour intervals are 2 m.

Additional file 7: Fig. S6 Computed results using the Hidaka (base) model at Oikamanai, Harashinai, and Masaki. The red circles show the tsunami deposit locations **a** found by Nanayama et al. (2002) in the Oikamanai pond and **b, c** those found by Takada et al. (2016) in Harashinai and Masaki. The solid contour denotes the topography. The dotted contour represents the bathymetry of fewer than 0 m. The contour intervals are 2 m.

Acknowledgements

We would like to thank Dr. Satoshi Kusumoto (Japan Agency of Marine-Earth Science and Technology) for his help in tsunami calculations. We are also grateful to Dr. Ryo Nakanishi (The University of Tokyo) for providing the fault parameters of the 1640 CE Mt. Komagatake tsunami simulation. We also would like to thank Enago (www.enago.jp) for the English language review. We used the plate isobath model proposed by Iwasaki et al. (2015), which was constructed from topography and bathymetry data by the Geospatial Information Authority of Japan (250 m digital map), Japan Oceanographic Data Center (500m mesh bathymetry data, J-EGG500, http://www.jodc.go.jp/jodcweb/JDOSS/infoJEGG_j.html), and the Geographic Information Network of Alaska, University of Alaska (Lindquist et al. 2004). We also used the GMT (Generic Mapping Tools) Versions 6.1.1 (Wessel et al. 2019) for data handling and plotting. For this study, we have used the computer systems of the Earthquake and Volcano Information Center of the Earthquake Research Institute, The University of Tokyo. We would like to thank the two editors (Prof. Ryota Hino and Eiji Ohtani), SeanPaul La Selle, and an anonymous reviewer for providing insightful comments that helped to improve this study.

Author contributions

KS conducted numerical simulations and wrote the manuscript. MY, DI, TI, and TB modified this manuscript and contributed to the discussion. All authors read and approved the final manuscript.

Funding

This research was supported by the Sasakawa Scientific Research Grant from the Japan Science Society (Daisuke Ishimura; No.2020 6001).

Availability of data and materials

We used open-source tsunami code JAGRUS (Baba et al. 2015) in <https://doi.org/10.5281/zenodo.3737816> and bathymetric data GtTM (Chikasada 2021) in <https://doi.org/10.17598/NIED.0021>.

Declarations

Competing interests

The authors declare that they have no competing interests.

Author details

¹Department of Earth and Planetary Science, The University of Tokyo, 7-3-1 Hongo, Bunkyo-ku, Tokyo 113-0033, Japan. ²Department of Geology, Faculty of Science, Shinshu University, 3-1-1 Asahi, Matsumoto, Nagano 390-8621, Japan. ³Department of Geography, Tokyo Metropolitan University, 1-1 Minami-Osawa, Hachioji, Tokyo 192-0397, Japan. ⁴International Research Institute of Disaster Science, Tohoku University, 468-1 Aoba, Aramaki, Aoba-ku, Sendai, Miyagi 980-8572, Japan. ⁵Graduate School of Technology, Industrial and Social Sciences, Tokushima University, 2-1 Minami-Jyosanjima, Tokushima 770-8506, Japan.

Received: 26 May 2022 Accepted: 1 December 2022

Published online: 22 December 2022

References

- Abe H, Sugeno Y, Chigama A (1990) Estimation of the height of the Sanriku Jogán 11 earthquake-tsunami (A.D. 869) in the Sendai Plain. *J Seismol Soc Japan* 43(2):513–525. https://doi.org/10.4294/zisin1948.43.4_513
- Abe T, Goto K, Sugawara D (2020) Spatial distribution and sources of tsunami deposits in a narrow valley setting-insight from 2011 Tohoku-oki tsunami deposits in northeastern Japan. *Prog Earth Planet Sci* 7:7. <https://doi.org/10.1186/s40645-019-0318-6>
- Aida I (1977) Simulations of large tsunamis occurring in the past off the coast of the Sanriku district. *Bull Earthq Res Inst Univ Tokyo* 52:71–101
- Aida I (1978) Reliability of a tsunami source model derived from fault parameters. *J Phys Earth* 26:57–73. <https://doi.org/10.4294/jpe1952.26.57>
- Baba T, Takahashi N, Kaneda Y, Ando K, Matsuoka D, Kato T (2015) Parallel implementation of dispersive tsunami wave modeling with a nesting algorithm for the 2011 Tohoku Tsunami. *Pure Appl Geophys* 172:3455–3472. <https://doi.org/10.1007/s00024-015-1049-2>
- Bricker JD, Gibson S, Takagi H, Imamura F (2015) On the need for larger Manning’s roughness coefficients in depth-integrated tsunami inundation models. *Coast Eng J* 57:1550005-1–1550005-13. <https://doi.org/10.1142/S0578563415500059>
- Chikasada N (2021) Global Tsunami Terrain Model. <https://kiyuu.bosai.go.jp/GtTM/>. doi:<https://doi.org/10.17598/NIED.0021>
- Ebina Y, Imai K (2014) Tsunami traces survey of the 1611 Keicho Ohshyu earthquake tsunami based on historical documents and traditions. *Rep Tsunami Eng* 31:139–148 (in Japanese)
- Goto K, Chagué-Goff C, Fujino S, Goff J, Jaffe B, Nishimura Y, Richmond B, Sugawara D, Szczuciński W, Tappin DR, Witter R, Yulianto E (2011) New insights of tsunami hazard from the 2011 Tohoku-oki event. *Mar Geol* 290:46–50. <https://doi.org/10.1016/j.margeo.2011.10.004>
- Goto K, Sugawara D, Abe T, Haraguchi T, Fujino S (2012) Liquefaction as an important source of the A.D. 2011 Tohoku-oki tsunami deposits at Sendai Plain, Japan. *Geology* 40:887–890. <https://doi.org/10.1130/G33123.1>
- Goto T, Satake K, Sugai T, Ishibe T, Harada T, Murotani S (2015) Historical tsunami and storm deposits during the last five centuries on the Sanriku coast, Japan. *Mar Geol* 367:105–117. <https://doi.org/10.1016/j.margeo.2015.05.009>
- Goto T, Satake K, Sugai T, Ishibe T, Harada T, Gusman AR (2019) Tsunami history over the past 2000 years on the Sanriku coast, Japan, determined using gravel deposits to estimate tsunami inundation behavior. *Sediment Geol* 382:85–102. <https://doi.org/10.1016/j.sedgeo.2019.01.001>
- Goto K, Ishizawa T, Ebina Y, Imamura F, Sato S, Udo K (2021) Ten years after the 2011 Tohoku-oki earthquake and tsunami: Geological and environmental effects and implications for disaster policy changes. *Earth-Sci Rev* 212:103417. <https://doi.org/10.1016/j.earscirev.2020.103417>
- Hatori T (1975) Tsunami magnitude and wave source regions of historical Sanriku tsunamis in northeast Japan. *Bull Earthq Res Inst Univ Tokyo* 50:397–414
- Hirakawa K, Nakamura Y, Nishimura Y (2005) Mega-tsunamis since last 6500 years along the Pacific coast of Hokkaido. *Spec Issue Chikyū Mon* 49:173–180 (in Japanese)
- Hirakawa K, Nakamura Y, Echigo T (1998) Tsunami Deposits on the Terrace Surfaces along the Pacific Coast of southern Tokachi, Hokkaido: Chronological and methodological significances. *Programs and Abstr, Seismol Soc Japan*, 2010 Fall Meet, C56. (in Japanese)
- Hokkaido Disaster Prevention Council (2012) Tsunami inundation map for the Pacific coast of Hokkaido. http://www.constr-dept-hokkaido.jp/sm/ktk/sim_tsunami/rep/00_report_zendou.html. Accessed 17 May 2022. (in Japanese)
- Iinuma T, Hino R, Kido M, Inazu D, Osada Y, Ito Y, Ohzono M, Tsushima H, Suzuki S, Fujimoto H, Miura S (2012) Coseismic slip distribution of the 2011 off the Pacific Coast of Tohoku Earthquake (M9.0) refined by means of seafloor geodetic data. *J Geophys Res Solid Earth* 117:B07409. <https://doi.org/10.1029/2012JB009186>

- Imai K, Maeda T, Iinuma T, Ebina Y, Sugawara D, Imamura F, Hirakawa A (2015) Pale tsunami source estimation by using combination optimization algorithm: case study of The 1611 Keicho earthquake tsunami. *Tohoku J Nat Disaster Sci* 51:139–144 (in Japanese)
- Ioki K, Tanioka Y (2016) Re-estimated fault model of the 17th century great earthquake off Hokkaido using tsunami deposit data. *Earth Planet Sci Lett* 433:133–138. <https://doi.org/10.1016/j.epsl.2015.10.009>
- Ishimura D (2017) Re-examination of the age of historical and paleo-tsunami deposits at Koyadori on the Sanriku Coast, Northeast Japan. *Geosci Lett* 4:11. <https://doi.org/10.1186/s40562-017-0077-4>
- Ishimura D, Miyauchi T (2015) Historical and paleo-tsunami deposits during the last 4000 years and their correlations with historical tsunami events in Koyadori on the Sanriku Coast, northeastern Japan. *Prog Earth Planet Sci* 2:16. <https://doi.org/10.1186/s40645-015-0047-4>
- Ishimura D, Miyauchi T (2017) Holocene environmental changes and paleo-tsunami history in Onuma on the southern part of the Sanriku Coast, northeast Japan. *Mar Geol* 286:126–139. <https://doi.org/10.1016/j.margeo.2017.01.011>
- Ishimura D, Ishizawa T, Yamada M, Aoki K, Sato K (2022) Washover deposits related to tsunami and storm surge along the north coast of the Shimokita Peninsula in the northern Japan. *Prog Earth Planet Sci*. <https://doi.org/10.1186/s40645-022-00529-9>
- Ishizawa T, Goto K, Nishimura Y, Miyairi Y, Sawada C, Yokoyama Y (2022) Paleotsunami history along the northern Japan trench based on sequential dating of the continuous geological record potentially inundated only by large tsunamis. *Quat Sci Rev* 279:107381. <https://doi.org/10.1016/j.quascirev.2022.107381>
- Iwasaki T, Sato H, Shinohara M, Ishiyama T, Hashima A (2015) Fundamental structure model of island arcs and subducted plates in and around Japan. In: AGU 2015 Fall Meet, San Francisco, Dec 14–18, T31B-2878
- Japan Meteorological Agency (2012) Report on the 2011 off the Pacific Coast of Tohoku earthquake. Technical report of the Japan meteorological agency 133, p 479
- Kajiura K (1963) The leading wave of a tsunami. *Bull Earthq Res Inst Univ Tokyo* 41:535–571
- Kase Y, Kawakami G, Koyasu H, Takahashi R, Sagayama T, Nishina K (2022) Event deposits recognized in the lowlands along the Tsugaru Strait, Hokkaido, Japan. *J Geol Soc Jpn* 128:7–26. <https://doi.org/10.5575/geosoc.2021.0035>
- Lindquist KG, Engle K, Stahlke D, Price E (2004) Global topography and bathymetry grid improves research efforts. *Eos Trans AGU* 85:186. <https://doi.org/10.1029/2004EO190003>
- Minoura K, Nakaya S (1991) Traces of tsunami preserved in inter-tidal lacustrine and marsh deposits: some examples from northeast Japan. *Jour Geol* 99:265–287. <https://doi.org/10.1086/629488>
- Minoura K, Hirano S, Yamada T (2013) Identification and possible recurrence of an oversized tsunami on the Pacific coast of northern Japan. *Nat Hazards* 68:631–643. <https://doi.org/10.1007/s11069-013-0640-z>
- Mitra R, Naruse H, Abe T (2020) Estimation of tsunami characteristics from deposits: inverse modeling using a deep-learning neural network. *J Geophys Res Earth Surface* 125:e2020JF005583. <https://doi.org/10.1029/2020JF005583>
- Mori N, Takahashi T, the 2011 Tohoku earthquake tsunami joint survey group (2012) Nationwide post event survey and analysis of the 2011 Tohoku earthquake tsunami. *Coast Eng J* 54:1250001-1–1250001-27. <https://doi.org/10.1142/S0578563412500015>
- Nagai R, Kikuchi M, Yamanaka Y (2001) Comparative study on the source processes of recurrent large earthquakes in Sanriku-oki Region: the 1968 Tokachi-oki earthquake and the 1994 Sanriku-oki earthquake. *Jour Seismol Soc Japan* 54(2):267–280. https://doi.org/10.4294/zisin.1948.54.2_267
- Nakamura Y (2016) Stratigraphy, distribution, and petrographic properties of Holocene tephra in Hokkaido, northern Japan. *Quat Int* 18:52–62. <https://doi.org/10.1016/j.quaint.2015.07.056>
- Nakamura W, Uchida N, Matsuzawa T (2016) Spatial distribution of the faulting types of small earthquakes around the 2011 Tohoku-oki earthquake: a comprehensive search using template events. *J Geophys Res Solid Earth* 121:2591–2607. <https://doi.org/10.1002/2015JB012584>
- Nakanishi R, Okamura S (2019) Tsunami deposits from the 1640 Hokkaido Komagatake eruption, north Japan: constraints on inundation heights and numerical simulation of volcanic debris avalanche-derived tsunami. *J Geol Soc Jpn* 125:835–851. <https://doi.org/10.5575/geosoc.2019.0032>
- Nakanishi R, Okamura S, Takashimizu Y, Sagayama T, Nishina K (2014) Distribution and origin of the 17th century tsunami deposit in Shiraoi, western Iburai Coast, Hokkaido, northern Japan. *Assoc Geol Collab Japan Monograph* 60:169–178
- Nomegaya Y, Satake K (2014) Reexamination of the A.D. 869 Jogan earthquake size from tsunami deposit distribution, simulated flow depth, and velocity. *Geophys Res Lett* 41:2297–2303. <https://doi.org/10.1002/2013GL058678>
- Nanayama F, Shigeno K (1998) Historical tsunami deposits on the Pacific coast of eastern Hokkaido along Kuril trench: an introduction. *Spec Issue Kaiyo Mon* 15:177–182 (in Japanese)
- Nanayama F, Shigeno K, Miura K, Makino A, Furukawa R, Satake K, Saito K, Sagayama T, Nakagawa M (2002) Evaluation of tsunami inundation limits from distribution of event deposits along the Kuril subduction zone, eastern Hokkaido: comparison of the Tokachi and Nemuro-Kushiro coasts. *Act Fault Paleoearthq Res Rep Geol Surv Jpn* 2:209–222
- Nanayama F, Satake K, Furukawa R, Shimokawa K, Atwater BF, Shigeno K, Yamaki S (2003) Unusually large earthquakes inferred from tsunami deposits along the Kuril trench. *Nature* 424:660–663. <https://doi.org/10.1038/nature01864>
- Nanayama F, Furukawa R, Shigeno K, Makino A, Soeda Y, Igarashi Y (2007) Nine unusually large tsunami deposits from the past 4000 years at Kiritappu marsh along the southern Kuril Trench. *Sediment Geol* 200:275–294. <https://doi.org/10.1016/j.sedgeo.2007.01.008>
- Naruse H, Abe T (2017) Inverse tsunami flow modeling including nonequilibrium sediment transport, with application to deposits from the 2011 Tohoku-Oki tsunami. *J Geophys Res Earth Surface* 122:2159–2182. <https://doi.org/10.1002/2017JF004226>
- Nishikawa T, Matsuzawa T, Ohta K, Uchida N, Nishimura T, Ide S (2019) The slow earthquake spectrum in the Japan Trench illuminated by the S-net seafloor observatories. *Science* 365:808–813. <https://doi.org/10.1126/science.aax5618>
- Nishimura Y, Miyaji N (1995) Tsunami deposits from the 1993 Southwest Hokkaido earthquake and the 1640 Hokkaido Komagatake eruption, northern Japan. *Pure Appl Geophys* 144:719–733. <https://doi.org/10.1007/BF00874391>
- Nishimura Y, Ishizawa T, Chiba T, Yokoyama Y, Miyairi Y (2020) Tsunami height distributions of the 1611 CE Keicho earthquake tsunami based on the tsunami deposits in Hokkaido. *Hist Earthq* 35:289
- Obara and Kato (2016) Connecting slow earthquakes to huge earthquakes. *Science* 353:253–257. <https://doi.org/10.1126/science.aaf1512>
- Cabinet Office (2020) The Committee for the model of a large earthquake along Japan Trench and Chishima Trench. https://www.bousai.go.jp/jishin/nihonkaiko_chishima/model/index.html. (in Japanese) Accessed 17 May 2022
- Okada Y (1985) Surface displacement due to shear and tensile faults in a half-space. *Bull Seismol Soc Am* 75:1135–1154
- Okamura Y, Namegaya Y (2011) Reconsideration of the 17th century Kuril multi-segment earthquake. *Act Fault Paleoearthq Res Rep Geol Surv Jpn* 11:15–20
- Satake K, Nanayama F, Yamaki S (2008) Fault models of unusual tsunami in the 17th century along the Kuril trench. *Earth Planets Sp* 60:925–935. <https://doi.org/10.1186/BF03352848>
- Sawai Y, Satake K, Kamataki T, Nasu H, Shishikura M, Atwater BF, Horton BP, Kelsey HM, Nagumo T, Yamaguchi M (2004) Transient uplift after a 17th-century earthquake along the Kuril subduction zone. *Science* 306:1918–1920. <https://doi.org/10.1126/science.1104895>
- Sawai Y, Kamataki T, Shishikura M, Nasu H, Okamura Y, Satake K, Thomson KH, Matsumoto D, Fujii Y, Komatsubara J, Aung TT (2009) Aperiodic recurrence of geologically recorded tsunamis during the past 5500 years in eastern Hokkaido, Japan. *J Geophys Res Solid Earth*. <https://doi.org/10.1029/2007JB005503>
- Sawai Y, Namegaya Y, Okamura Y, Satake K, Shishikura M (2012) Challenges of anticipating the 2011 Tohoku earthquake and tsunami using coastal geology. *Geophys Res Lett* 39:1–6. <https://doi.org/10.1029/2012GL053692>
- Sawai Y, Namegaya Y, Tamura T, Nakashima R, Tanigawa K (2015) Shorter intervals between great earthquakes near Sendai: scour ponds and a sand layer attributable to A.D. 1454 overwash. *Geophys Res Lett* 42:4795–4800. <https://doi.org/10.1002/2015GL064167>

- Sugawara D (2021) Numerical modeling of tsunami: advances and future challenges after the 2011 Tohoku earthquake and tsunami. *Earth-Science Rev* 214:103498. <https://doi.org/10.1016/j.earscirev.2020.103498>
- Sugawara D, Goto K, Imamura F, Matsumoto H, Minoura K (2012) Assessing the magnitude of the 869 Jogan tsunami using sedimentary deposits: prediction and consequence of the 2011 Tohoku-oki tsunami. *Sediment Geol* 282:14–26. <https://doi.org/10.1016/j.sedgeo.2012.08.001>
- Suwa Y, Miura S, Hasegawa A, Sato T, Tachibana K (2006) Interplate coupling beneath NE Japan inferred from three-dimensional displacement field. *J Geophys Res Solid Earth* 111:B04402. <https://doi.org/10.1029/2004J B003203>
- Takada K, Shishikura M, Imai K, Ebina Y, Goto K, Shin K, Yamamoto H, Igarashi A, Ichihara T, Kinoshita H, Ikeda T, Iwate Prefecture Government River Division Department of prefectural Land Development (2016) Distribution and ages of tsunami deposits along the Pacific Coast of the Iwate Prefecture. *Act Fault Paleoearthq Res Rep Geol Surv Jpn* 16:1–52
- Takashimizu Y, Sagayama T, Nishina K, Oka T, Nakamura Y, Nishimura Y (2007) A 17th-century tsunami deposits discovered on the eastern Iburi Coast, Hokkaido, northern Japan. *Quatern Res* 46:119–130. <https://doi.org/10.4116/jaqua.46.119>
- Takashimizu Y, Nishina K, Kawakami G, Sato Y, Nakanishi R, Tamura M, Hirose W, Takahashi R, Ishimaru S (2017) Identification of a 17th-century tsunami deposit on the northern Hidaka coast, Hokkaido, northern Japan. *Quatern Res* 56:1–9. <https://doi.org/10.4116/jaqua.56.1>
- Tanigawa K, Sawai Y, Shishikura M, Namegaya Y, Matsumoto D (2014) Geological evidence for an unusually large tsunami on the Pacific coast of Aomori, northern Japan. *J Quat Sci* 29:200–208. <https://doi.org/10.1002/jqs.2690>
- Tanioka Y, Satake K (1996) Tsunami generation by horizontal displacement of ocean bottom. *Geophys Res Lett* 23:861–864. <https://doi.org/10.1029/96GL00736>
- Tanioka Y, Nishimura Y, Hirakawa K, Imamura F, Abe I, Abe Y, Shindou K, Matsu-tomi H, Takahashi T, Imai K, Harada K, Namegawa Y, Hasegawa Y, Hayashi Y, Nanayama F, Kamataki T, Kawata Y, Fukasawa Y, Koshimura S, Hada Y, Azumai Y, Hirata K, Kamikawa A, Yoshikawa A, Shiga T, Kobayashi M, Masaka S (2004) Tsunami run-up heights of the 2003 Tokachi-oki earthquake. *Earth Planets Sp* 56:359–365. <https://doi.org/10.1186/BF03353065>
- Tetsuka H, Goto K, Ebina Y, Sugawara D, Ishizawa T (2020) Historical and geological evidence for the seventeenth-century tsunamis along Kuril and Japan trenches: implications for the origin of the AD 1611 Keicho earthquake and tsunami, and for the probable future risk potential. *Geol Soc Lond*. <https://doi.org/10.1144/sp501-2019-60>
- Tohoku Electric Power (2016) Progress report on the safety evaluation of the Higashidori nuclear power plant concerning tsunami: case study of interlocking earthquake from Nemuro-Oki, Tokachi-Oki to northern Sanriku-Oki. https://www.tohoku-epco.co.jp/electr/genshi/safety/topics/pdf/20160428_1.pdf. Accessed 17 May 2022 (in Japanese)
- Tsuji Y, Ueda K (1995) Evaluation of Sanriku earthquake tsunamis, 1611 CE Keicho, 1677 CE Empo, 1763 CE Horeki, 1793 CE Kansei, 1856 CE Ansei Sanriku Tsunamis. *Hist Earthq* 11:75–106 (in Japanese)
- Tsuji Y, Mabuchi Y, Ooie T, Imamura F (2011) Trace height investigations of Keicho 16 Sanriku earthquake tsunami in Iwate Prefecture. *Rep Tsunami Eng* 28:173–180 (in Japanese)
- Tsuji Y, Imai K, Mabuchi Y, Ooie T, Okada K, Iwabuchi Y, Imamura F (2012) Field survey of the Tsunami of the 1677 Empo Boso-Oki and the 1611 Keicho Sanriku-Oki Earthquake. *Rep Tsunami Eng* 29:189–207 (in Japanese)
- Tsuji Y, Mabuchi Y, Okada K, Kuroyanagi Y, Kinami T, Matsuoka Y, Sato M, Haga Y, Imamura F (2014) Height distributions of the tsunamis accompanied with the 1677 North Sanriku-oki, the 1763 Hachinohe-oki, and the 1856 North Sanriku-oki earthquakes on the coast of the north part of Tohoku district. *Rep Tsunami Eng* 31:149–199 (in Japanese)
- Usami T, Ishii H, Imamura T, Takemura M, Matsuura R (2013) Materials for comprehensive list of destructive earthquakes in Japan 599–2012. Univ Tokyo Press, Tokyo (in Japanese)
- Utsu T (1999) Seismicity studies: a comprehensive review. Univ Tokyo Press, Tokyo (in Japanese)
- Utsu T (2004) Catalog of damaging earthquakes in the world (through 2002), Tokyo. http://iisee.kenken.go.jp/utsu/index_eng.html. Accessed 11 Apr 2022
- Watanabe H (1998) Comprehensive list of tsunamis to hit the Japanese Islands, 2nd edn. Univ Tokyo Press, Tokyo (in Japanese)
- Watanabe M, Nakata T, Suzuki Y, Koiwa N (2012) Co-seismic uplift submarine active fault around northwestern end of Shimokita Peninsula, northeast Japan. *Act Fault Res* 36:1–10. https://doi.org/10.11462/af.2012.36_1
- Wessel P, Luis JF, Uieda L, Scharroo R, Wobbe F, Smith WHF, Tian D (2019) The generic mapping tools version 6. *Geochem Geophys* 20:5556–5564. <https://doi.org/10.1029/2019GC008515>
- Yamanaka Y, Tanioka Y (2022) Short-wave and run-ups of 1611 Keicho tsunami along the Sanriku Coast. *Prog Earth Planet Sci* 9:37. <https://doi.org/10.1186/s40645-022-00496-1>

Publisher's Note

Springer Nature remains neutral with regard to jurisdictional claims in published maps and institutional affiliations.

Submit your manuscript to a SpringerOpen® journal and benefit from:

- Convenient online submission
- Rigorous peer review
- Open access: articles freely available online
- High visibility within the field
- Retaining the copyright to your article

Submit your next manuscript at ► [springeropen.com](https://www.springeropen.com)
